Colorimetric Detection of ssDNA using DNA-functionalized Gold Nanoparticles

by

Michael Keng-Wei Lam

A thesis submitted in partial fulfillment of the requirements for the degree of

Master of Science

Department of Chemistry
University of Alberta

Abstract

Remarkable progress has been made in terms of developing gold nanoparticle (AuNP) based colorimetric systems for biodiagnostics. There are two general strategies: the target analyte triggers assembly leading to a color change from red solution to blue precipitated AuNPs; the target analyte triggers disassembly of pre-formed aggregates leading to a blue to red color change. As colorimetric detection systems suitable for point-of-care applications should be rapid, this dissertation will systematically address the effects of temperature on the rate of target DNA induced disassembly of DNA-AuNP aggregates in DNA detection.

Specifically in Chapter 2, DNA-AuNP aggregates (purple) composed of two AuNP probes hybridized with a complementary linker DNA sequence are disassembled into colloidal DNA-AuNPs (red) with the addition of a target DNA sequence fully complementary to the linker. By monitoring the disassembly upon addition of target at various temperature settings, we observe an increasingly rapid disassembly as we near the melting temperature (T_m).

Using the protocols developed from this system, we introduce a single-stranded overhang (toehold) into the linker to increase the rate of target-triggered disassembly and systematically varied the overhang length while monitoring the temperature-dependence of target-triggered disassembly. The length of the overhang greatly influences the temperature sensitivity of the target-triggered disaggregation process. For toehold lengths of 5 bases, rapid target-triggered disassembly occurs even at room temperature (Chapter 3). In addition, we explore strategies for making

this colorimetric process suitable for shelf storage by lyophilization of the pre-formed DNA-AuNP aggregates containing 5 base overhangs on the linker. We vary the storage temperature of the solid (lyophilized) DNA-AuNP aggregates which can be resuspended and used to detect target DNA colorimetrically.

Preface

This thesis is the original work by Michael Lam. Some of the research was collaborative with other members of the Gibbs-Davis Group and will be stated below.

Dr. Delwar Sikder provided some guidance at the onset of the project described in Chapter 2, and DNA conjugated gold nanoparticles were left as a gift upon his graduation and used for preliminary experiments. I was responsible for the data collection and analysis of the results included in the chapter. Loading thiolated DNA onto gold nanoparticles was a protocol adapted from Dr. Abu Kausar. Portions of this chapter appear in a manuscript that is currently under review. Dr. Julianne Gibbs-Davis proposed the project, and Dr. Julianne Gibbs-Davis and Dr. Tendai Gadzikwa (visiting researcher) extensively edited the manuscript that was used as a basis for this chapter.

Preliminary kinetic measurements based on the toehold mediated strategy described in Chapter 3 were performed by Trang Nguyen, an undergraduate student performing a CHEM 401 project in our lab. Upon determining a successful system, all data collection and duplicates were performed by me. Additionally, Safeenaz Alladin-Mustan worked on this project coupling it to an amplification system which was not included in this thesis. Dr. Tendai Gadzikwa aided in the analysis of the data and wrote a substantial portion of the manuscript, which was used as the basis for parts of this chapter. All of the material in Chapter 2 and data from chapter 3 before the lyophilization experiments comprises the submitted manuscript pending review.

The preliminary lyophilization experiments and initial data collection was performed by me. Currently, duplicates of the lyophilized experiments are being measured jointly by me and Wanyue Xu, an undergraduate student performing a CHEM 299 project in our group. This project was supervised by Dr. Julianne Gibbs-Davis who also edited the paper that was used for parts of this chapter.

Acknowledgements

I would like to take this chance to express my gratitude and thanks to my advisor Professor Julianne Gibbs-Davis for her patience and guidance throughout my two-year journey. Despite some times when I have not been my best, she has taken the strength to motivate, inspire and kindle the flame of scientific learning. Her penchant to detail in and out of the lab has been of great value and is greatly appreciated. I have been privileged to be in one of the most dedicated and hard working groups which has trained me to become self-reliant and increasingly inquisitive.

I would also like to thank my committee and defense examination members, Professor Michael Serpe, Professor Christopher Cairo and Professor Mark McDermott for valuable suggestions, enthusiasm and encouragement in improving my research.

I would also like to thank Dr. Eric Kool for his thought-provoking insight into Chapter 3 of the project. Additionally, I would like to extend my appreciation for the past and present group members of the Gibbs-Davis Group. In particular, Delwar Sikder, Abu Kausar, Eiman Osman, Safeenaz Alladin-Mustan, Sun Kim, Zhiguo Li, Akemi Darlington and Benjamin Rehl. I wouldn't have been able to do it without the vital support and encouragement from everyone.

Finally, I would like to thank my parents and my brother for providing constant love and support. Thank you for teaching me the value of hard work, dedication and always inspiring me to be my best.

Table of Contents

List of Figures

List of Tables

Chapter 1 – Biomolecule-Functionalized AuNP for Molecular Recognition

1.1.1 – Introduction to Gold Nanoparticles

Scientists have made great strides over the last two decades in developing and synthesizing novel nanomaterials in physical dimensions on the order of 1-100 nm. One of the most captivating of these materials are gold nanoparticles (AuNPs) which have spawned and developed simple to complex applications over these years. One example of their growing impact is illustrated in their current article count as of the year 2000, a total of 800 articles were published regarding this topic. However, to date, there are a total of 180,000 and more articles within this field. Nanomaterials, in particular gold, have been highly regarded in the last couple decades owing to their unique features including intense optical properties, easy fabrication and high stability.[1,2] One unusual property of AuNPs is their surface plasmon resonance (SPR), which is the collective oscillations of electrons that occur upon absorbing light in a narrow range in the visible. The localized SPR results in AuNPs having high extinction coefficients that can exceed organic dyes by as many as 3 orders of magnitude.[3,4] Many properties of these nanomaterials are dependent on the size shape and composition which ultimately determines their function, absorption and behavior in various applications. Consequently, researchers have synthesized AuNPs in varying shapes and sizes which allow for use in applications ranging from catalysis, colorimetric detection, and theranostics (therapeutics and diagnostics in a single agent) based on their optical behavior respectively in the UV, visible, and near infrared range.[5] For example, 13-nm diameter AuNPs absorb maximally at a wavelength of ~ 519 nm resulting in a wine-red color for AuNP dispersions. Upon aggregation, these

materials undergo a redshift with an extinction maxima at ~ 540 nm, leading to a blue/purple appearance. Moreover, these aggregates have a tendency to precipitate from solution. This visual change of AuNPs based on aggregation is important in many colorimetric detection platforms (Figure 1.1).[2,6]

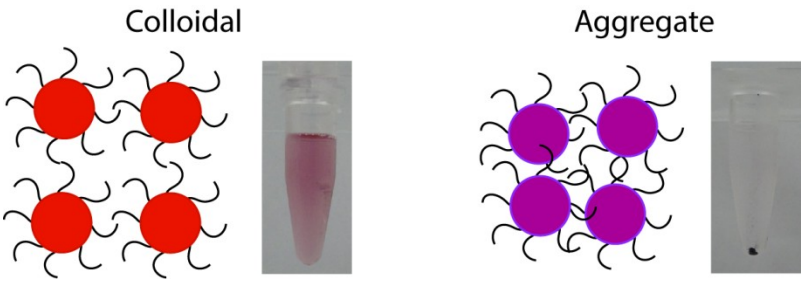

Figure 1.1. Colloidal gold compared to aggregated gold as a vivid colorimetric detection platform.

Other unique features of AuNPs include their high quenching properties while in close proximity to many fluorophores. This ability to quench fluorescence has been exploited in applications using molecular beacon type systems, whereby at one end a DNA sequence is attached to the surface of AuNPs while the other end contains a fluorophore. Upon formation of a hairpin loop, the fluorophore is brought in close proximity to the AuNP, effectively quenching any fluorescent activity. However, if complementary DNA binds to the hairpin, the hairpin is forced apart and the distance between the AuNP and fluorophore is great enough to allow for fluorescence.[7]

The ease of AuNP preparation is another major advantage of using these materials; the Turkevich method developed in 1951 is the most common strategy, which, leads to reproducible syntheses of monodisperse 13 nm AuNPs.[8,9] In 1973, Frens was able to expand this synthetic method by varying the $HAuCl_4$, reducing

agent and ligand ratio allowing for nanoparticles size ranges of 16 to 150 nm. Modern methods of syntheses have been able to fine tune AuNPs into various anisotropic shapes including nanocubes,[10] rods,[11,12] prisms[13] and wires,[14] ultimately changing their structure and function. Due to the small sizes of AuNPs (13 nm), the surface to volume ratio of nanomaterials allows for close to a hundred different anchoring points for surface functionalization.[12] Moreover, the versatility of these materials are further demonstrated by the diversity of ligands that are capable of stabilizing AuNPs such as citrate, phosphine, phosphine oxides, thiols, amines and carboxylates.[15]

In detection applications, AuNPs have become one of the most widely used sensor materials. General strategies involve the conjugation of probe molecules to the nanoparticle surface to attain high specificity to molecular biomarkers. As the capping agents used to synthesize AuNPs are not typically the participants in biomolecular recognition, ligand exchange reactions are necessary in a dual function of stabilizing the AuNP surface and providing functionality. The most commonly used ligands are typically thiolated ligands due to the strong Au-S interaction when forming a monolayer on the AuNP surface. While the bond strength of C-C bonds are typically on the order of ~85 kcal/mol, the Au-S bond has been estimated to be ~45 kcal/mol, a stable semi-covalent bond.[16] Negatively charged functional groups like DNA will also exhibit weak electrostatic interactions with the AuNP, however, upon removal of these charged groups, stability of the AuNPs are disrupted and aggregation can occur. Therefore, thiolated linkers are most often employed as an intermediary linker between the functional group of interest and the AuNP surface.[17]

As a result of their accessibility, functionalized AuNPs can potentially be used in point-of-care (POC) systems, where POC is a diagnostic test that is performed outside the clinical setting, due to their high stability, inexpensive syntheses, easy functionalization and unique optical properties.[18] Detection methods such as colorimetric, fluorescence, surface enhanced raman spectroscopy and various electrochemical enhancement platforms have been well documented with these materials.[19] The focus of this chapter will be addressing applications of AuNPs in colorimetric diagnostic applications and the current research initiatives towards point-of-care (POC) applications as it is most pertinent to this thesis.

1.1.2 - Introduction and Motivation for Point of Care (POC) Devices in Diagnostic Testing

Point of care devices have been ever increasing over the past decade. Finding colorimetric reporters, like AuNPs sensors, in the early detection and subsequent monitoring of diseases has proven to be of dire importance in reducing the impact and improving the survival rate in patients. One of the key attributes of diagnostic tests tailored for a clinical setting is the accuracy and sensitivity of the assay.[20] However, due to high turnaround times, sophisticated instrumentation and lack of skilled worker training, such options are often not available in developing countries and non-centralized settings. On the other hand, many advantages come with using point of care (POC) devices such as their low cost, rapid output, robustness, no/low power consumption and portability.[21] Their importance comes into play in many settings

including those where clinical facilities are nonexistent (warzones or disasters), where there are low resources (developing countries) and where timing is critical (emergency situations).[22]

1.1.3 - Introduction to Lateral Flow Assays

One of the most widely used tests currently in the POC setting are lateral flow assay (LFA) tests. LFAs have been around for a long time with the first prototype developed in 1951 by Singer and Plotz in the diagnosis of rheumatoid arthritis.[23] LFAs are typically simple devices that detect the presence of an analyte in a sample through the transport of fluid through a polymer most commonly, nitrocellulose. LFAs are typically composed of four main components: a sample pad, a conjugate pad, a detection pad and an absorbant pad (Figure 1.2). The sample pad is typically where the sample is applied and as it travels through the membrane by capillary action, it is able to enter into the conjugate pad and bind a colorimetric reporter reagent. Further along the strip, antibodies are immobilized on the target line of the strip resulting in retention of the colorimetric reporter. A control line is typically included where antibodies are immobilized to ensure proper wicking of the colorimetric agents. Finally, the absorbent pad is used for the proper steady wicking of the sample.

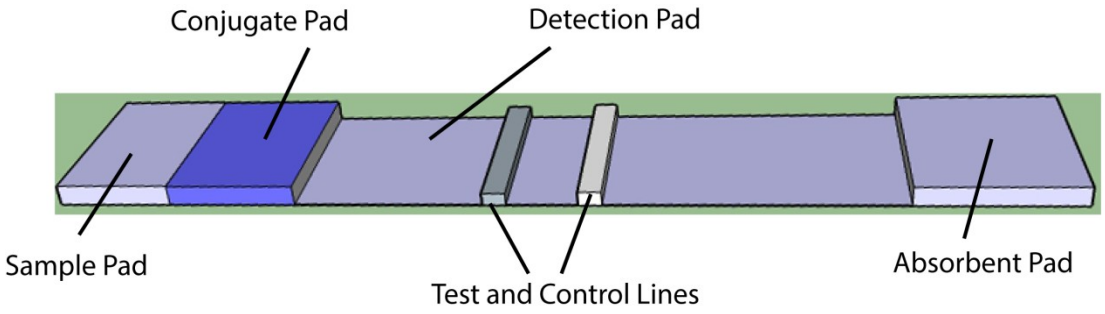

Figure 1.2. A general construct of an LFA consisting of a sample pad, conjugate pad, detection pad (with control and test lines) and an absorbent pad. The sample is drawn towards the absorbent pad through capillary action.

Despite the relatively simple construction of LFAs, they present multiple advantages such as being relatively inexpensive, durable (long shelf life), portable and fast.[24] The speed of LFAs is in contrast with most conventional laboratory testing techniques that have a large turnaround time leading to increased treatment times. The rising importance and need for LFAs in point of care tests in disease detection and health assessments have arisen in the past decade particularly in developing countries. The World Health Organization has set up a criterion for ideal POCs that address this disease burden: a test should be affordable, specific, sensitive, user-friendly, rapid, robust, equipment free and deliverable to end-users (ASSURED). In colorimetric testing for POC tests, many different colorimetric reporters have been used in detecting a target substrate such as latex beads and quantum dots. Among the list of colorimetric materials, AuNPs are the most widely used and most popular,[25] due to the stability of gold in solid or solution. AuNPs are also easily conjugated and are relatively inert.

Although LFAs coupled with AuNPs may not achieve the entire criterion, it certainly attains a fair amount of the principles.[26] One of the major drawbacks of LFAs, however, are that they are considerably constrained by sensitivity, particularly for nucleic acid based detection. Therefore, coupling LFAs to various amplification techniques is key to it becoming a realizable platform. For early disease detection, nucleic acid tests (NATs) are typically the most effective tests.[27] NATs are generally composed of a detector sequence typically linked to a reporter such as AuNPs and a capture probe that is complementary to the (amplified) target sequence to elicit a colorimetric response.[24] Polymerase chain reaction (PCR) is still the "gold standard" in terms of the conventional amplification method of DNA. One of the requirements for PCR is a thermocycler, which is an onerous requirement for remote or low-resource regions. As a result, there has been a shift towards isothermal amplification methods for POC applications such as loop mediated DNA amplification (LAMP)[28] or rolling circle amplification (RCA).[29] To illustrate, a study by Hu et al. detected HIV specific sequences using DNA functionalized AuNPs that would subsequently bind to the immobilized sequence on the target line, with a sensitivity of 0.25 nM.[30] Another successful demonstration of a nucleic acid biosensor was shown by Zeng and coworkers in detecting human genomic DNA; they were able to combine nucleic acid sequence based amplification (NASBA), an isothermal amplification technique, whereupon the target sequence was amplified then subsequently detected using an LFA leading to a detection limit of 0.01 fM.[27] One of the current drawbacks of this system is that it costs approximately $5 - $20 per test.[31] Another drawback is that while this system is isothermal at room temperature, it required a total of 2.5 hours to

obtain a result. Alternative schemes for detecting DNA colorimetrically that do not require the preparation of lateral flow tests will be discussed in section 1.2.3.

1.2- Colorimetric Detection of Biomolecules with Au-NPs

1.2.1 - Antibody linked Gold Nanoparticles (Ab-AuNPs) for Colorimetric Detection

Clinical testing has relied heavily on enzyme linked immunosorbent assays (ELISA) since it was first described in 1971 by Engvall and Perlman.[32] Conventional ELISA tests are typically designed to detect antigens or antibodies by immobilization onto a well via direct or sandwich assay strategies. By coupling antibodies with enzymes that react with chromogenic substrates, color change ensues (figure 1.3).

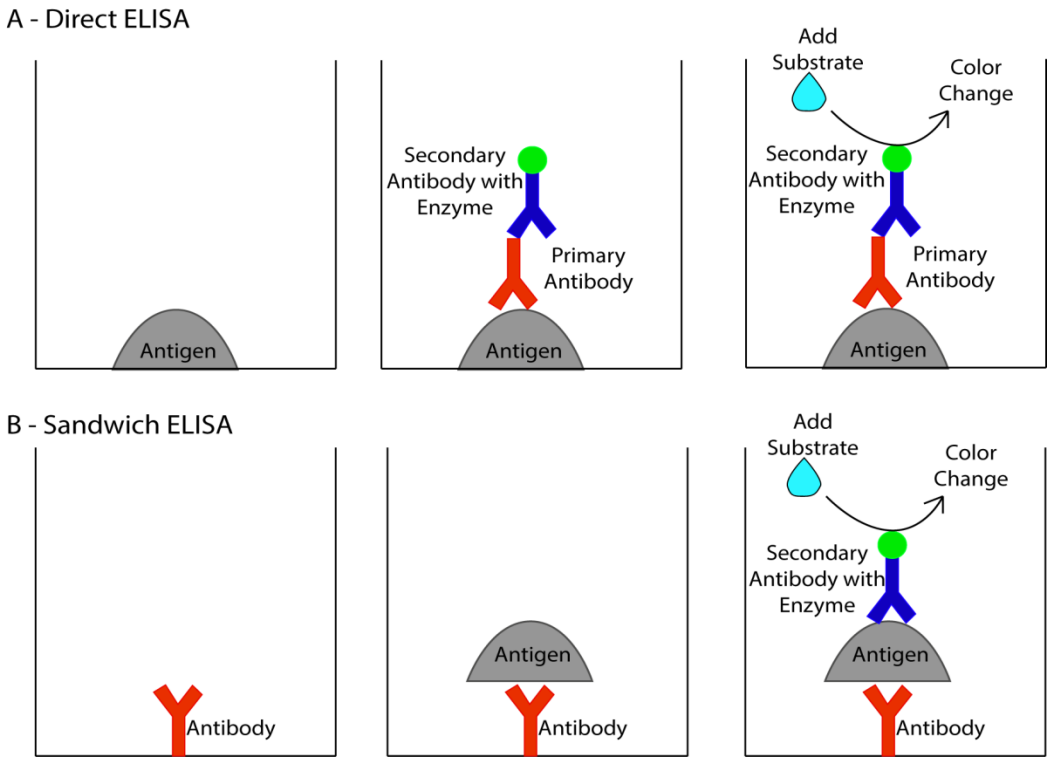

Figure 1.3. Schematic illustrating detection of primary antibody in sample via direct ELISA and detection of antigen via sandwich ELISA. (A) The antigen is initially immobilized and the primary antibody from sample attaches, if present, and upon washing, secondary antibody is applied with enzyme that catalyzes a substrate to illicit color change. (B) Antibody is initially immobilized and antigen from sample attaches if present, upon washing, secondary antibody is applied with enzyme to catalyze a substrate for color change.

For many immunoassays, AuNPs have replaced the need for enzyme conjugation on antibodies.[33] Enzymes are being replaced with AuNPs as a colorimetric reporter because enzymes can be expensive to conjugate and must be stored in temperature and pH stable environments. Additionally AuNP immunoassays are often more sensitive. For example, even in the common

pregnancy test, conjugation of two sets of AuNPs with primary and secondary antibodies can detect human chorionic gonadotropin (hCG) with a 25 pg/mL detection limit compared with the 300 pg/mL limit in conventional ELISA kits utilizing horseradish peroxidase (HRP).[34] Additionally, reports of whole blood immunoassays using Ab-AuNP based detection of antibodies using aggregation based colorimetric detection has shown great success making them superior to conventional ELISA as it removes the need for enzymes in detection. Single step methods utilizing AuNPs have also led to sensitive immunoassays. For example, Liu and coworkers have demonstrated the feasibility of detecting influenza A in an optimized aggregation based system in 30 minutes without the need for instrumentation or enzymes. Even more recently, amplification based methods using human serum analysis for cardiac troponin I has been demonstrated with silver staining of bound Ab-AuNPs in a sandwich assay with a turnaround time of 1.5 hours compared to traditional ELISA of 3 hours.[35] While the analysis of human biological samples still rely on ELISA, the transition towards AuNPs as a reporter has been well documented in screening studies.[33] Although antibodies are still the gold standard of recognition (probe) materials, replacement with aptamers, a nucleic acid analogue of antibodies, is has been foreseen to have inherent advantages over antibodies.[25]

1.2.2 Analyte Detection of Non-DNA Targets using Nucleic Acid-Functionalized Gold Nanoparticles for Colorimetric Detection

As mentioned, another strategy for adding biorecognition properties to AuNPs involves functionalizing them with aptamers, a DNA sequences that can bind a specific antigen, ion, or other small molecule. Such sequences are obtained from a library and selectively enriched in a process known as SELEX (systematic evolution of ligands by exponential enrichment).[36] DNA sequences that are systematically enriched to specifically bind a ligand with high binding constants ($K_d = 10^{-8}$-10^{-9}) are taken from a random library of as many as 10^{15} sequences.[37] Many examples of aptamers that have been discovered through SELEX are known which bind to heavy metals,[38] small molecules like cocaine,[39] peptides,[40,41] toxins,[42] cells and bacteria.[43] By tethering these antibody analogues to AuNPs, not only can one exploit the unique optical properties of AuNPs but each probe carries the function and specificity associated with aptamers. One of the drawbacks with aptamers, however, is that they require much time to isolate and purify through SELEX. Yet, once selected, they can be synthesized with reproducibility and in large quantities for high throughput use. In comparison, each batch of monoclonal antibodies required cumbersome and expensive isolation and characterization.[25] Antibodies are also intolerant to temperatures unlike aptamers that reversibly fold and are therefore tolerable of high temperatures making them an attractive alternative.[25,44] However, one disadvantage of aptamers is their susceptibility to DNAases which can become an issue. A specific class of aptamers are DNAzymes, DNA sequences capable of enzymatic properties such as cleavage of oligonucleotides. DNAzymes are derived in the similar fashion

to aptamers, however, the analyte now becomes a specific cofactor (typically metal ion) that is required for the DNAzyme to become activated and functional.[37,45,46]

Monitoring the levels of heavy metal in the environmental is especially important as contaminated drinking water is detrimental to human health. As a result, many studies have examined ways of utilizing AuNPs as a colorimetric detection platform.[46,47] As mentioned, one of the most magnificent properties of AuNP is their ability to reversibly aggregate and disassemble leading to colorimetric changes.[48] The stability of functionalized AuNP is due to the capping ligand that is surrounding the AuNP shell, which influences the surface potential. By increasing the potential, the capping ligand limits inter-particle interactions and prevents aggregation.[49] Many factors are able to disrupt the delicate balance of AuNP colloids such as variation in salt concentration,[50] electrostatic effects, pH and temperature.[51] Single-stranded DNA is an excellent stabilizer and prevents the aggregation of AuNPs due to its highly negative charge. However, upon hybridization with a complementary strand, the electrostatic interactions between the DNA and surface of the AuNP are disrupted resulting in aggregation of the AuNPs.

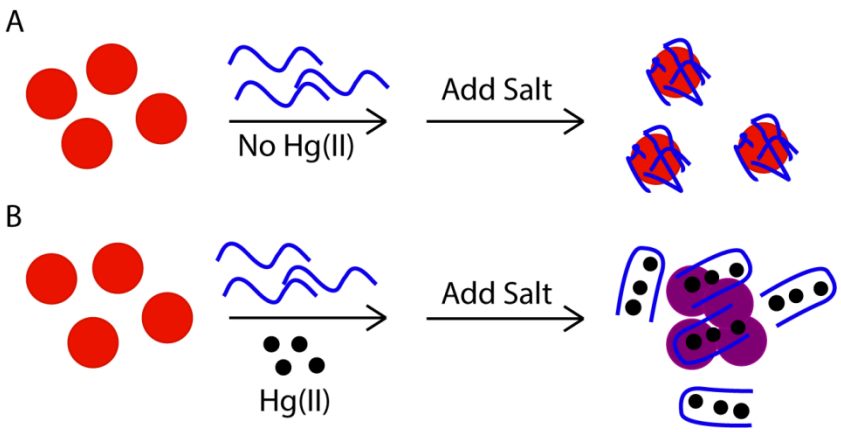

Figure 1.4. (A) The addition of salt to citrate capped AuNPs in the presence of poly-thymidine DNA results in physisorption of DNA which prevents aggregation. (B) In the presence of Hg^{2+}, favorable thymine-Hg-thymine bonds form preventing the DNA from physisorbing on the AuNPs. As a result, upon salt addition, aggregation ensues due to insufficient surface stabilization of AuNPs.[47]

Another example where nanoparticle aggregation was triggered is through the interactions with single-stranded DNA involving the detection of Hg^{2+} using a thymine rich sequence. Polythymidine readily loops around to form a stem loop in the presence of Hg^{2+} ions based on thymine-Hg-thymine interactions. Initially, citrate capped colloidal AuNP is stabilized by poly-thymidine ssDNA in solution, however, upon the addition of Hg^{2+}, the ssDNA forms a hairpin loop, reducing the surface charge stabilization with AuNPs in solution. Consequently upon salt addition AuNPs will aggregated.[52] Lead detection using citrate capped AuNPs in basic pH (11.2) has also been developed where the presence of Pb^{2+} ions would form complex coordination in the form of $Pb(OH)_3^-$ with citrate, leading to destabilization of the surface charge of AuNPs and causing them to aggregate.[53] Other examples include

gallic acid stabilized AuNPs in a similar fashion and the exploitation of AuNP surface stability for detection for the detection of Pb^{2+}.[47]

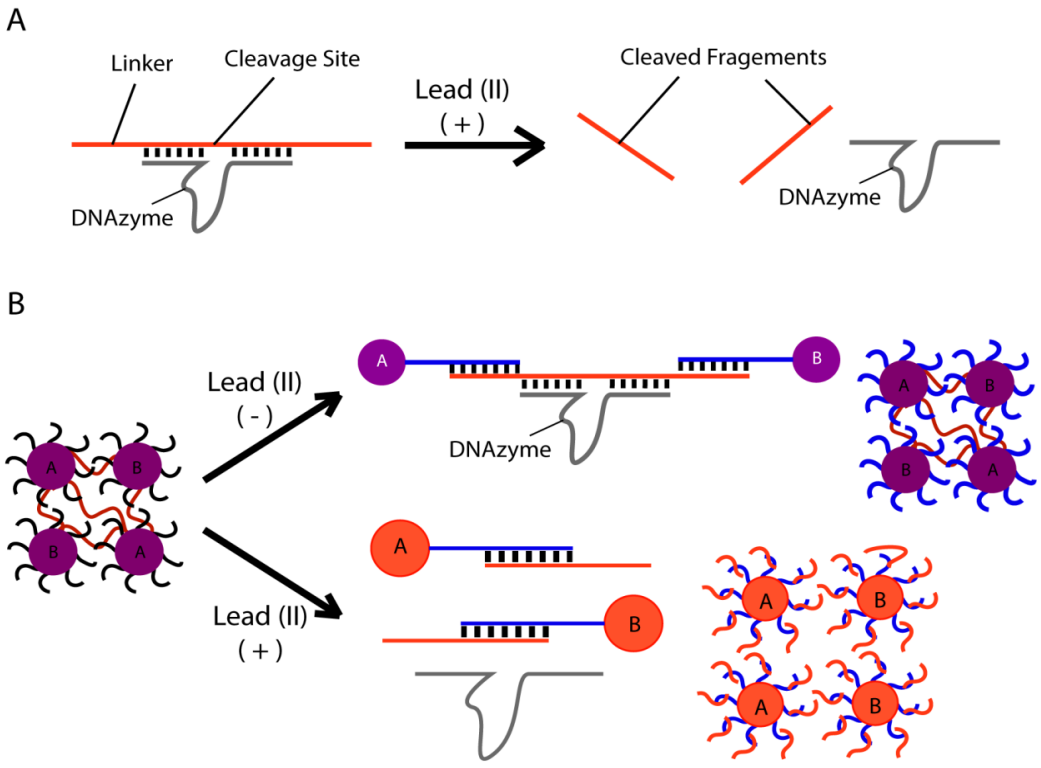

Figure 1.5. (A) Illustration of DNAzyme cleaving the linker strand in the presence of Pb^{2+}. (B) When the two DNA-AuNP and DNAzyme are partially hybridized to the linker strand, aggregates form with the quadruplex. In the absence of Pb^{2+}, DNA-AuNP, remain tethered together (purple). In the presence of Pb^{2+}, the active DNAzyme cleaves the linker strand and DNA-AuNPs are dispersed (red).[54]

A heavy metal ion study by Liu and Lu that involved using DNA-functionalized gold nanoparticles modified with a thiolated DNAzyme, a DNA

sequence with cleaving properties that allowed for the detection of Pb^{2+}. First the DNAzyme sequence hybridized with a linker strand to form AuNP aggregates. The addition of Pb^{2+} activated the DNAzymes causing it to cleave the linker and cause disassembly of aggregates, as Pb^{2+} was the essential cofactor for the DNAzyme to function. In the absence of Pb^{2+}, the DNAzyme remained inactive and the DNA-AuNP mixture remained aggregated.[54,55] Significantly, colorimetric change was observed in less than 10 minutes with a detection limit of 5 μM Pb^{2+}.

In the realm of small molecule diagnostics, interesting strategies utilizing LFAs have been shown for adenosine detection. A report by Liu and coworkers revealed how size exclusion of AuNP aggregates could be applied in LFA platforms. First, aggregated aptamer-functionalized AuNPs that also contained biotin modifications were conjugated with the membrane. Then in the presence of adenosine, binding would occur with the aptamer, which triggered disassembly of the aggregates. Next, diffusion of the AuNPs through the membrane occurred until they were captured by streptavidin on the target line. In the absence of target, the aggregates would be unable to diffuse through the pores and no response was elicited.[37,56,57]

1.2.3 DNA Detection in Aggregation Based Schemes for Colorimetric Detection using DNA Functionalized Gold Nanoparticles

AuNPs functionalized with thiolated DNA has been shown to produce highly specific and tunable colorimetric sensors for DNA targets as well. As a result, interest

in utilizing AuNPs as a POC colorimetric reporter for nucleic acid tests has expanded over the last decade.[58] The earliest utilization of DNA functionalized AuNPs as a colorimetric platform was reported in 1996 when the Mirkin group successfully functionalized AuNPs with thiolated DNA in a way that exhibited unusual melting and optical properties. In their study, AuNPs were synthesized using citrate capped 13 nm AuNPs and incubated with thiolated DNA. Two sets of these AuNP probes were functionalized with thiolated DNA and designed to be placed tail to tail.

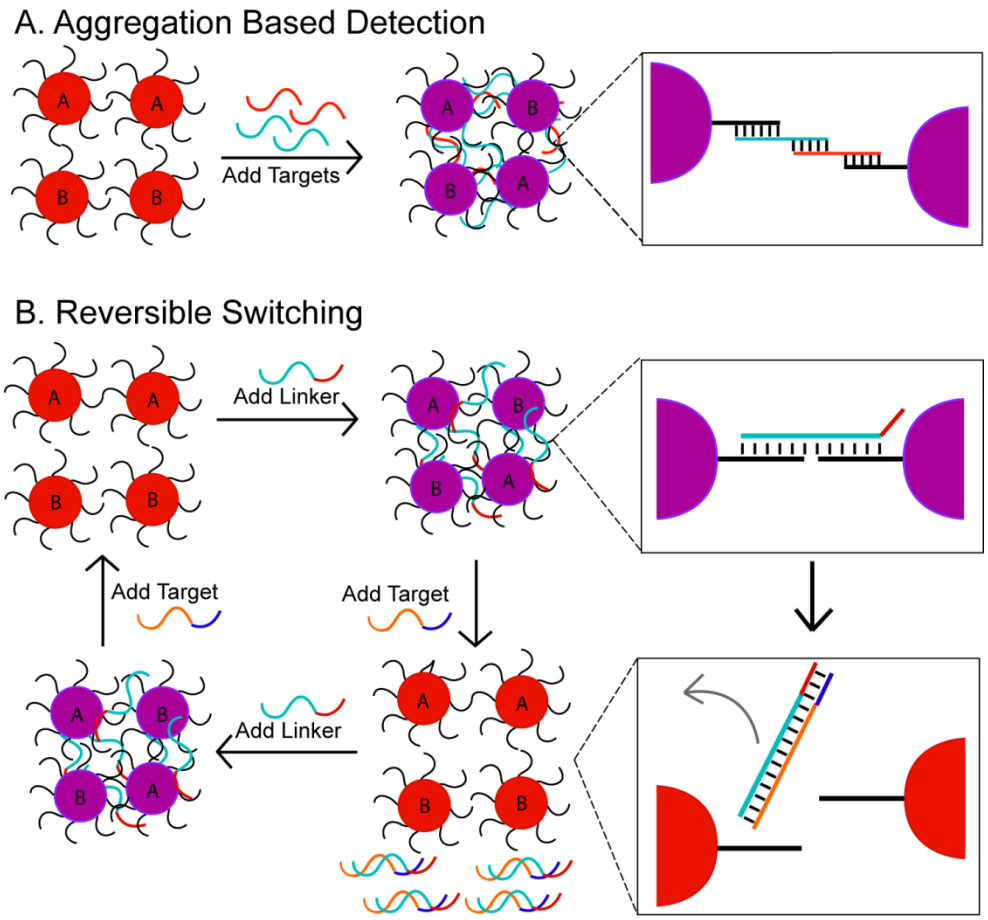

Figure 1.6. (A) Scheme illustrating Mirkin group's first use of functionalized DNA-AuNP assays where target addition of two target strands with partial overlapping regions to each other and to two half complementary AuNP probes elicited aggregation.[59] (B) Niemeyer and coworkers demonstrated the reversible nature of colloidal and aggregated DNA-AuNP with incremental and successive addition of linker and target.[48]

Two linker strands are then added which are half complementary to each other and the AuNPs thereby bridging the two sets of probes together to obtain dark purple aggregates as a result of the closing distance between the AuNPs. Consequently, this

results in the surface plasmon resonance broadening and red shifting, which can be followed with the naked eye or using UV-visible spectroscopy (Figure 1.6A). Interestingly, in subsequent studies, they demonstrated the bridging of AuNP probes with a target strand and after hybridization and heating, the melting temperature (T_m) observed was incredibly sharp compared with free DNA. Unlike normal melted duplex DNA, which exhibits a broad melting transition, aggregated DNA-AuNP complexes exhibit a very narrow temperature transition, a consequence of the high DNA packing on the AuNP surface.[60] This physical property is known as cooperativity, where the displacement of one DNA strand in the aggregate assembly destabilizes other target strands upon heating.[61-63] While this is not an intrinsic property of DNA nor AuNP individually, when combined, these unique properties allow for various detection platforms that would not be otherwise possible. An example of this is in SNP detection, because of the intrinsic thermal sensitivity of DNA-linked AuNP aggregates, single base mismatches could be elucidated confidently.[64] Interestingly, in a paper following this system, spotting AuNP aggregates or colloids onto a TLC plate can result in a permanent red or purple spot qualitatively detecting the presence or absence of a target.[64] One of the drawbacks, however, was the relatively long wait times to achieve aggregation. Still, aggregation based assays were the first DNA-AuNP based systems for DNA detection; their introduction to DNA detection marked an important advancement, which paralleled and even exceeded the performance of conventional colorimetric probes in many systems.[2,6]

Eight years later, Niemeyer and coworkers demonstrated the reversible nature of AuNP aggregates by initially linking two AuNP probes together with a linker strand, which contained an overhang, a region that is not base paired to the probes. The addition of a complementary target strand to the linker strand enabled disassembly of AuNP aggregates due to the formation of a more stable duplex and the unbridging of aggregates (Figure 1.6B).[48] This process was repeatable by sequentially adding linker leading to aggregation, followed by target leading to disassembly. One important aspect of this example is it illustrated that the addition of DNA could be used to trigger disassembly as well as assembly of DNA-modified gold nanoparticles.

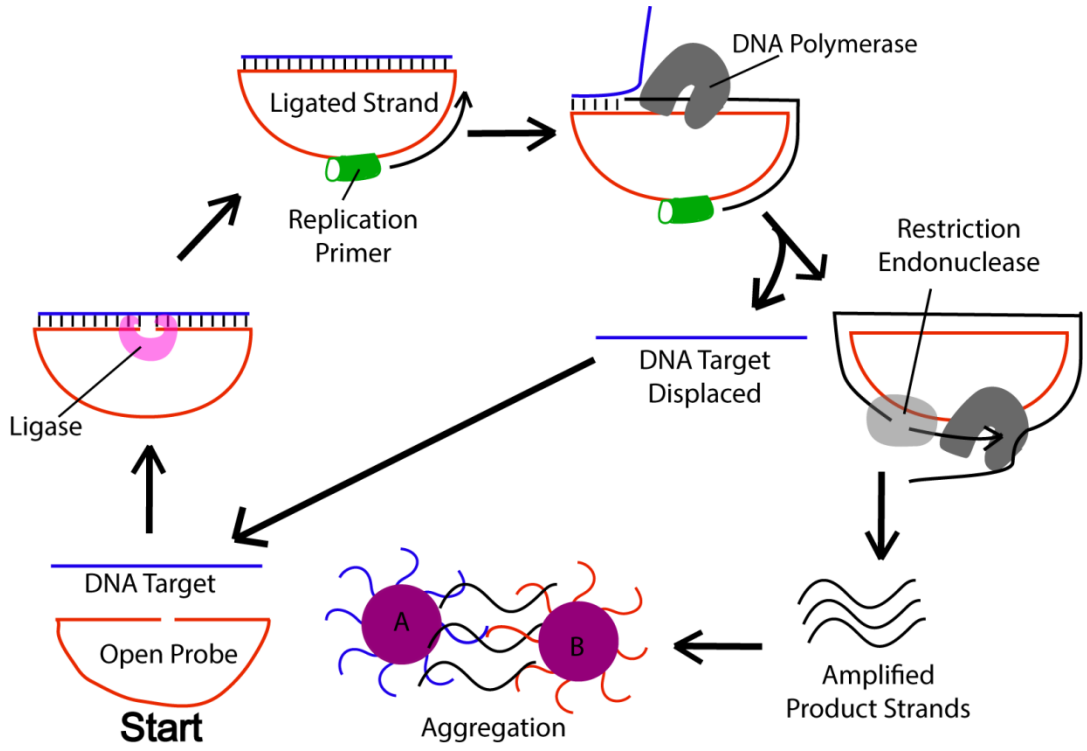

Figure 1.7. Schematic illustrating rolling circle amplification (RCA) coupled with aggregate-based detection. First the open probe hybridizes with DNA target bringing the ends of the open probe into close proximity for ligation. Upon ligation, a

replication primer attaches and the strand is elongated by DNA polymerase. In the process of elongation, the target strand is displaced and recycled for another round of hybridization. In the continuous elongation by DNA polymerase, restriction endonuclease cuts at restriction sites to form identical product fragments. These product fragments when mixed with DNA-AuNP probes A and B elicit aggregation.[65]

To increase the sensitivity of aggregation-based assays, Li et al. coupled rolling circle amplification (RCA),[66] an isothermal amplification technique, with target-triggered AuNP aggregation. This colorimetric detection method was used to detect a sequence specific for the β-thalassemia, a hereditary disease affecting hemoglobin function.[65] The assay was sensitive to point mutations and had a limit of detection of 70 fM. One of the highlights of this paper was that no other sophisticated instrumentation was required for this assay. However, one of the drawbacks was that it was more suited for the clinical setting as it required 4 hours for complete detection and the isothermal temperature at which the test was performed was at 37 °C, necessitating heating instrumentation.

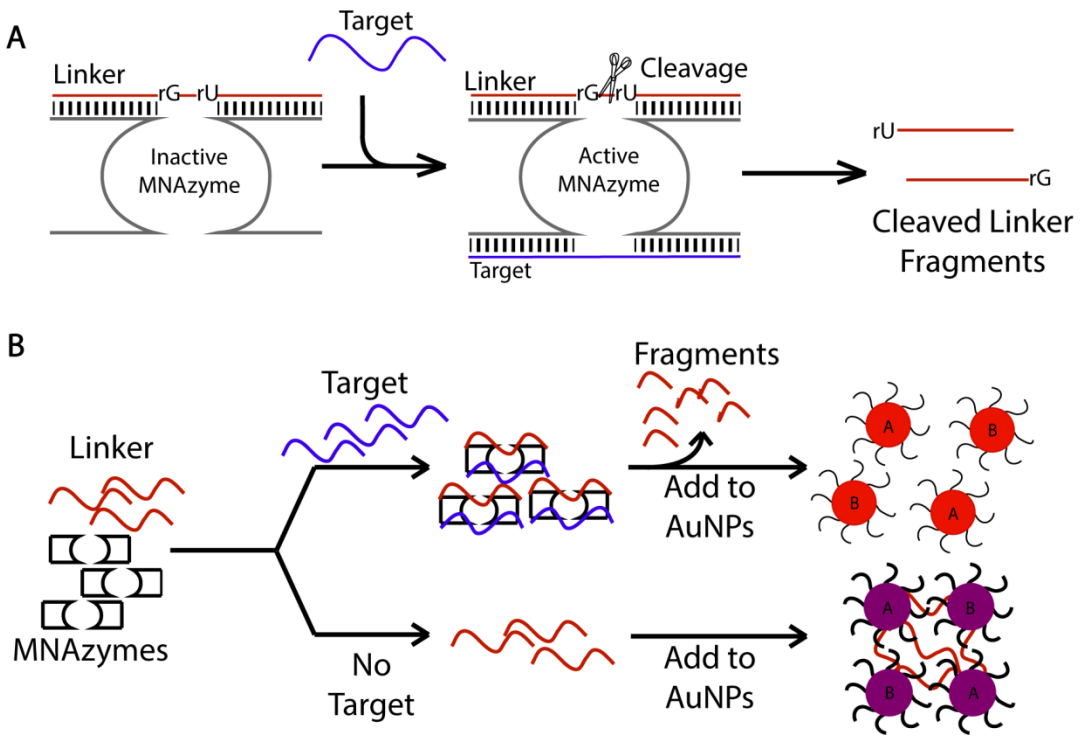

Figure 1.8. (A) Illustration of linker strand cleavage in the presence of target strand due to activation of an MNAzyme. (B) Scheme illustrating the presence and absence of target. If target is present, MNAzyme will cleave the linker. Upon the subsequent addition of DNA-AuNPs, the cleaved linker strands will be unable to bridge and aggregate the NPs. If no target is present, the uncleaved linker strands bridge DNA-AuNPs and aggregate them.[45]

Recently, Zagarovsky and Chan demonstrated the detection of infectious diseases with the use of a DNAzyme cleavage amplification in a POC assay. Initially, they synthesized two sets of multicomponent nucleic acid enzyme (MNAzyme) that contained half complementary sequences to a linker strand and target at different places of the DNA sequence (Figure 1.8A). Introduction of target to these MNAzyme and linker mixtures induced a conformation change and the subsequent cleavage of the substrate linker (Figure 1.8A). DNA-AuNPs were then added to the system but

the cleaved linkers could not assemble the DNA-AuNPs into aggregates and therefore the solution remained red. However, in the absence of target, the uncleaved linker is able to bridge the AuNP probes causing the AuNPs to aggregate. One of the most exciting implications of this study is that by tailoring the DNA sequence of the MNAzyme catalytic probe sequences, selectivity of the cleavage can only occur on complementary linker strands. Moreover, when multiple targets (gonorrhea, malaria, syphilis and hepatitis) were mixed together and placed with their respective MNAzymes sequences, it was highly sequence specific, allowing multiple parallel target detection.[45] In addition to its high specificity, they were able to perform this assay in 1 hour and obtaining a modest limit of detection of 30 pM at an isothermal temperature of 50 °C. Despite its need for heating equipment, one of the major highlights in their work was illustrated by the lyophilization of the MNAzymes and linker strands together for future use, resulting in a robust, yet simple assay.

1.2.4 DNA Detection in Disassembly Based Schemes for Colorimetric Detection using DNA-Functionalized Gold Nanoparticles

Recently, the reverse process using DNA-AuNP disassembly in colorimetric detection has proven to be an elegant platform for colorimetric sensing. One of the major advantages of disassembly compared to aggregation is that it involves a "turn-on" assay (the emergence of bright red) compared to a "turn off" system (bright red to dull purple/blue aggregates, which is more subtle to observe). Moreover, this

approach has been shown to be rapid as demonstrated by various disassembly studies.[67] As mentioned, the reversible nature of DNA-AuNPs is not a new concept as it was first shown by Niemeyer and coworkers in 2004.[48] However, it was not until 2013 when researchers first used DNA-AuNPs aggregates as a disassembly method in the presence of target DNA as a colorimetric detection method.[68] Although DNA-AuNP disassembly assays were known for the colorimetric detection ions and small molecules[56] (as detailed in section 1.2.2) there are still only a limited number of reports using disassembly of DNA-AuNPs as a method for DNA detection. One such report was recently published by Trantakis et al. where they demonstrated direct target disassembly of AuNP aggregates sensitive to a one base pair mismatch.

\

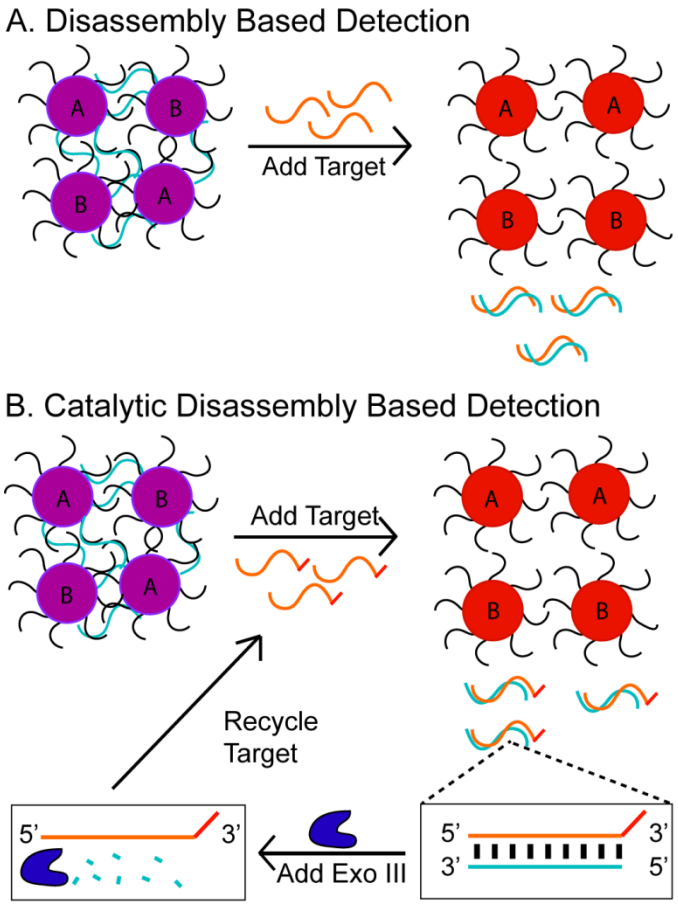

Figure 1.9. (A) One of the first disassembly based assays for the detection of DNA using target induced disassembly of DNA-AuNPs with pre-formed aggregates.[69] (B) Illustration of a catalytic disassembly system involving the Exonuclease III digestion of the 3' blunt end of one strand of the duplex DNA causing the recycling of target DNA in the disassembly of pre-formed AuNP aggregates.[68]

One potential drawback of their system was that it took almost 3 hours for complete disassembly with a sensitivity of 300 nM when the assay was performed at room temperature.[69] Zhou et al. optimized the idea by introducing toeholds in various positions and of various lengths on the linker strand. However, at best there approach required 20 minute to achieve disassembly of half of the aggregates, making the

detection step quite slow and required elevated temperatures. However, with the coupling to exonuclease III, the target strand was recycled and further displacement of the linker was possible, leading to a detection limit of 2 nM. Unfortunately, with the addition of enzymatic cleavage of blunt ends for recycling of target strands, the detection assay increased to 2 hours.[68] One of the most recent studies by Duan et al. utilized DNA target-triggered disassembly of AuNPs as the read-out method for a strand displacement cascade. As with the other two systems, this method also suffered the drawbacks of a relatively slow disassembly although it did operate at room temperature.

Assembly based detections schemes have been widely developed for many assays such as small molecules, cells, DNA, protein. The same is not true for disassembly based DNA detection systems. DNA detection using DNA-AuNPs has only been recently explored in a disassembly based method and has proven to be a potential candidate in colorimetric platforms. Until this work, however, disassembly had not proven to be a rapid method for DNA detection.

1.2.5 Thesis Overview

While there is certainly room for improvement, the amount of progress in colorimetric detection of DNA utilizing DNA-AuNPs has been monumental. In the field of diagnostics using AuNPs, progress in developing an AuNP device that truly works at room temperature, is affordable, robust and sensitive is still a challenge. One possibility is using disassembly based systems to achieve these goals.

Chapter 2 explores the work of conjugating thiolated linker DNA that bridges to two sets of 13 nm AuNPs in an attempt to understand the temperature dependence in target-triggered disassembly of the pre-formed aggregates. While much work had focused on parameters such as the effect of salt concentration,[50] pH, gaps and linker lengths,[70,71] on the thermal stability of AuNP aggregates, no one had systematically studied the influence of temperature on strand displacement leading to aggregate dissolution. Indeed, most studies have performed DNA-AuNP disassembly assays at one temperature without focusing on the kinetics of disassembly.[68,69] Therefore, by varying the temperature, we explored the optimal temperature at which disassembly occured for these pre-formed aggregates and found it to be 2 °C below the aggregate dissoluction, or melting, temperature. In addition, as we decreased the temperature further to T_m –4, 6 and 8 °C, we found that the disassembly rate decreased dramatically and at the lowest temperatures did not yield a colorimetric response upon target addition when at decreased temperatures.

In chapter 3, we explored a way to increase the temperature range over which disassembly could work (ideally including room temperature) using DNA AuNP aggregates that also contained non base-paired region at the end of the linkers (known as toeholds or overhangs). We systematically determined the influence of target-triggered disassembly kinetics as a function of toehold length and temperature. By varying the toehold length, we found that we were able to tune the temperature at which disassembly could overlap with room temperature in a colorimetric disassembly assay that works under 10 minutes. Specifically, we found that an ideal length would be approximately 5-7 bases on each side resulting in a colorimetric

assay that was still rapid 10 °C less than the T_m of the aggregates. In addition, we demonstrated the feasibility of utilizing these materials without any instrumentation by adding target to aggregates on the bench followed by light shaking by hand to elicit a colorimetric response in less than 10 minutes. Finally, in an effort to demonstrate the robustness of these materials, we lyophilized the DNA-AuNP aggregates with toeholds and stored the solid aggregates at various temperatures from -20 °C to 40 °C. Upon resuspension and target addition on the benchtop, we found that these materials retained their biosensing capabilities and integrity even after harsh temperature treatment in the solid state. In all cases the resuspended aggregates disassembled rapidly providing a vivid colorimetric response.

Finally, this thesis will conclude with short remarks on the advances of disassembly based systems and the subsequent directions with particular relevance to POC applications.

Chapter Two: Rapid Colorimetric Detection of ssDNA By Controlling the Temperature of Target Triggered Disassembly of DNA-linked Gold Nanoparticles.

2.1 Introduction

In the past two decades there has been a surge of interest in the use of gold nanoparticles (AuNPs) in the detection of biomolecular and environmental targets such as DNA,[72-74] proteins[73,75] and metal ions.[54,55] One of the most remarkable aspects of AuNPs that has made them excellent sensor materials is their ability to be covalently functionalized with recognition agents like DNA.[2] Not only are such materials simple to prepare, but hybrid DNA-AuNP conjugates are extremely selective nucleic acid probes able to distinguish between a one base-pair mismatch and a perfectly complementary target using thermal stringency washes.[64] This selectivity of DNA-AuNPs stems from their unique thermal sensitivity, which is exemplified by the extremely sharp thermal dissociation, or melting, transitions of duplex linked DNA-AuNP aggregates. The origin of this sharp melting of duplex-linked AuNP aggregates is attributed to cooperative interactions between neighboring duplexes as well as the phase behavior of the aggregate.[57,63,68,71]

In the realm of nucleic-acid based diagnostics, one of the major challenges that remains is finding a method which offers a simple, specific, yet rapid platform for usage in a point-of-care (POC) setting.[76,77] Owing to their advantageous optical properties, DNA-modified AuNPs are promising candidates for nucleic acid POC assays as target induced AuNP aggregation causes a color change from red to

purple/blue. However, one disadvantage of aggregation-based DNA bio-sensing is that it can take more than 8 hours for complete aggregation of DNA-AuNPs by target hybridization.[69,78] Consequently, strategies for increasing the rate of aggregation have been explored, such as decreasing the entropy of the probe DNA strands by rigidifying their points of attachment to the nanoparticle surface.[62]

Although aggregation of DNA-AuNPs by hybridization is intrinsically a slow process, dissociation is not (vide infra).[38] Therefore, we reasoned that rapid colorimetric detection should be possible using the presence of target DNA to trigger disassembly rather than assembly of AuNPs if the conditions were optimal. In contrast to the most common strategy of detection by target-induced aggregation, strand displacement triggered disassembly would render colorimetric detection rapid enough that it could be applied for point-of-care diagnostics (Figure 2.1). As reported by Sturla and co-workers the method of target-induced disassembly remained quite slow, requiring wait times of more than 6 hours for complete disassembly with a detection limit of 300 nM. In contrast, here we demonstrate how target induced disassembly can be rapidly achieved in 10 minutes or less allowing for simple colorimetric detection of DNA down to low nM concentrations by carefully tuning the assay temperature to facilitate strand displacement.

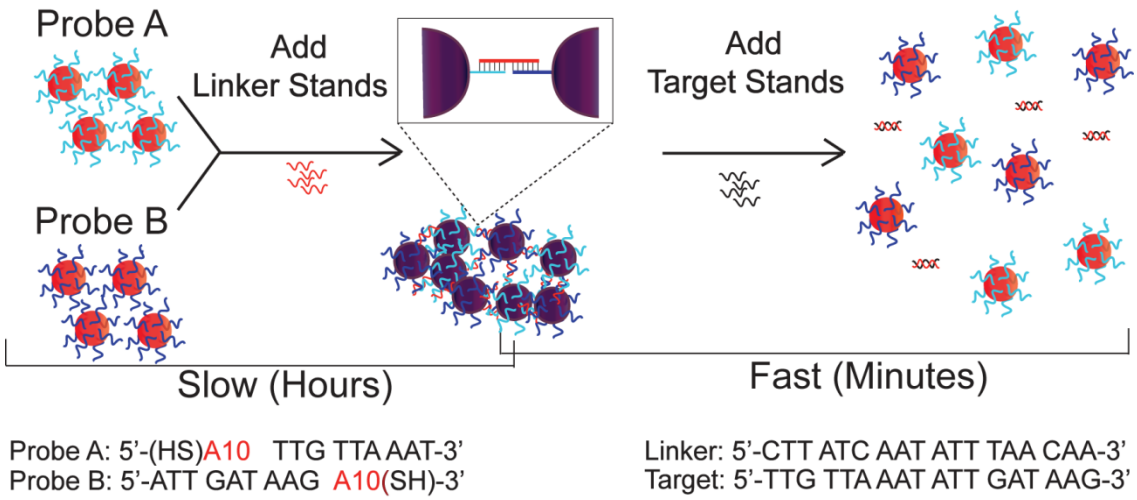

Figure 2.1. Schematic illustrating Probe A and Probe B functionalized AuNPs, half complementary to a *linker* strand, which hybridizes with the linker over hours. Upon the addition of *target*, the target strands bind the linker strand preferentially liberating the AuNP probes on the order of minutes.

2.2 Experimental

2.2.1 DNA Syntheses and Characterizations

All reagents were purchased from Glen Research to synthesize DNA strands by solid-phase synthesis. Solid-phase synthesis was performed on an Applied Biosystems Model 392 DNA/RNA Synthesizer. Concentration calculations were conducted on an HP 8453 diode-array spectrophotometer equipped with a HP 89090A Peltier temperature controller. All DNA concentrations were determined from their absorbance at λ = 260 nm and extinction coefficients determined by Oligocalc.[79] Additionally, all samples, buffers, solutions were dissolved in MilliQ water (18.1ΩM)

Following DNA synthesis, samples were either deprotected overnight with 1 mL NH_4OH at room temperature or quickly deprotected with 1 mL NH_4OH at 65°C for 2 hours. The strands were then purified using a DMT-On procedure with Glen-Pak Cartridges (Glen Research, Catalogue # 60-5200-01). All bases used to synthesize DNA were standard nucleotide phosphoramidites. Additionally, Thiol-Modifier C6 (10-1936-90) and 3' Thiol-Modifier C3 S-S CPG (Catalogue # 20-2933-41) were used to synthesize thiolated strands. Purified DNA was lyophilized before placing in the freezer for future use.

Table 2.1. DNA sequences

Probes	**DNA Sequences and Modifications**
Probe A:	5'- S-C6*- AAA AAA AAA ATT GTT AAA T-3'
Probe B:	5'- ATT GAT AAG AAA AAA AAA A *C3-S-3'
Linker:	5'-CTT ATC AAT ATT TAA CAA-3'
Target:	5'-TTG TTA AAT ATT GAT AAG-3'

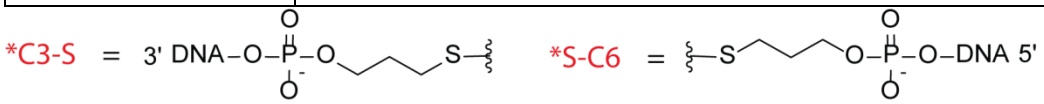

2.2.2 Gold Nanoparticle Synthesis

Gold nanoparticles with 13 nm diameter were synthesized following the established Turkevich Synthesis.[8,9,64] Briefly, all glassware used in the synthesis was soaked in aqua regia and then washed multiple times with milliQ water and then oven dried at ~100 °C before use. Generally, $HAuCl_4 \cdot 3H_2O$ (0.0985 g, 0.25 mmol) purchased from Sigma-Aldrich (CAS # 16961-25-4) was dissolved in MilliQ water

(250 mL) and then placed in a round bottom flask with a stir bar and heated to reflux. After 20 minutes, an aqueous solution of trisodium citrate (25 mL, 38.8 mM) was added to the refluxing Au solution. Immediately after adding the trisodium citrate solution, the reaction mixture changed from a light yellow, to black and then a dark wine-red color. This mixture was allowed to reflux for another 10 minutes followed by cooling and filtering through a polyethersulfone (PES) filter unit pore size of 0.45 μM (Catalogue # 10040-462, VWR). The nanoparticles were stored in a plastic container in the dark at room temperature. The nanoparticles were characterized by UV-vis absorbance spectroscopy revealing the characteristic peak at λ = 519 nm of citrate capped 13-nm gold nanoparticles.[70]

2.2.3 DNA Loading on Gold Nanoparticles

The loading of thiolated DNA to gold nanoparticles followed the procedure of Hurst et al. with a few modifications.[50] Briefly, thiolated DNA was generated by reacting the disulfide terminated strand at room temperature with a dithiothreitol (DTT) solution (0.1 M DTT, 0.18 M PBS, pH 8) for 2 hours and then purified by passing through a PD-10 desalting column (GE Healthcare, Catalogue # 17-0851-01) with PBS (50 mM PBS, 0.05% SDS, 2.5 % NaN_3 pH = 7 buffer) (Catalogue # 17-0851-01, GE Healthcare) and collected in fractions. The amount of thiolated DNA in each fraction was determined from UV-Vis absorbance monitoring at 260 nm. The fractions containing thiolated DNA were then combined, vortexed for 5 seconds, table top centrifuged and then monitored again at 260 nm. This thiolated DNA (1.5 pmol) was then added to AuNPs (1 mL, ~1.5 x 10^{12} particles/mL), 3 mL of water, and buffer

(50 mM PBS, 0.05 wt% SDS, 2.5 wt % NaN_3, pH 7) to make a total of 5 mL. Next, this mixture was salted up to 0.05 M NaCl by adding increments of 2 M NaCl buffer (2 M NaCl, 10 mM PBS, 0.01% SDS, 0.5% NaN_3, pH 7) before leaving the solution to sit for at least 1 day. Thereafter, the mixture was further salted up to 0.5 M NaCl in 0.1 M NaCl increments using the 2 M NaCl buffer. Samples were also sonicated ~15 seconds in between salt addition. Upon reaching the desired salt concentration, samples were incubated for at least two days before purification.

2.2.4 Purification and Hybridization of Gold Nanoparticles

After two days (or more) of incubation of the DNA-AuNP after reaching the highest salt concentration (0.5 M NaCl), the purification of these AuNP probes was performed as outlined by Hurst et al. with slight modification.[50] Briefly, the AuNP probe solution was placed in several 2 mL eppendorfs and centrifuged at 14000 RPM for 30 minutes. Afterwards, each eppendorf was decanted of supernatant to remove free DNA and the AuNPs resuspended in buffer (0.5 M NaCl, 10 mM PBS, 0.01 wt% SDS, 0.5 wt% NaN_3, pH 7). These steps were repeated 3 times. After purification, the concentration of gold nanoparticles was determined through UV-visible absorbance spectroscopy by monitoring at 525 nm (λ_{max}) and the concentration was determined using a molar absorptivity coefficient ε of 2.4 x 10^8 $M^{-1}cm^{-1}$.[50,72] After determining the concentration of gold nanoparticles for both probe A and probe B, 1.5 pmol of each, with respect to AuNP, was placed in an 1.7-mL eppendorf followed by 60 pmol of linker, which then filled to a final volume of 1 mL with buffer (0.5 M NaCl, 10mM PBS, 0.01% SDS, 0.5% NaN_3, pH 7). This colloidal mixture was then

placed at room temperature for a minimum of one day before use to allow the duplex-linked aggregates to form.

2.2.5 Kinetic and Thermal Denaturation Experiments

Kinetic experiments were conducted with hybridization mixtures prepared as stated above. The room temperature aggregates were pipetted into a 1-mL cuvette containing a stirbar, placed into the temperature-controlled spectrophotometer and stirred at 200 rpm. The absorbance was then monitored at 525 nm with background subtraction at 850 nm at 30 second intervals for 3600 seconds. After the aggregate mixture equilibrated for 1200 seconds at the desired temperature, varying amounts of target (60 pmol, 30 pmol, 15 pmol, 5 pmol and 0 pmol) was added in 5 μL of buffer and the absorbance was monitored for the remaining 2400 seconds. Thermal denaturation experiments were also performed on similar aggregate samples while stirring at 200 rpm with a temperature ramp from 25 °C until 55 °C with a 1 °C increment and a 1 minute hold time.

2.3 Results and Discussion

2.3.1 Experimental Design

To develop a rapid strand displacement assay, AuNPs of 13-nm diameter were first synthesized and functionalized with thiol-terminated DNA according to the literature.[70,80] Upon functionalization, we prepared two different sets of AuNPs with sequences complementary to two adjacent regions on a linker sequence, such that the linker strand bridged two AuNPs together upon hybridization. As a result of the

many DNA strands attached to each AuNP, hybridization of the two types of AuNPs with the linker led to the formation of dark purple aggregates over the span of hours. To further illustrate this phenomenon, we monitored overnight the extinction at 525 nm to determine the time required to achieve full aggregation (Figure 2.2A).

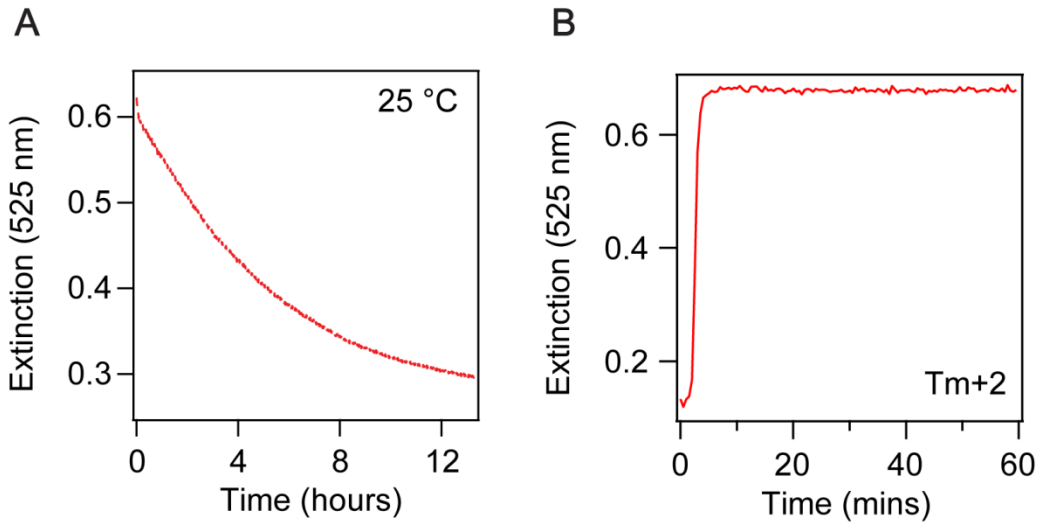

Figure 2.2. Kinetic study of aggregation (A) and disassembly (B) monitored at λ = 525 nm as a function of time to contrast the rate at which assembly and disassembly occur. (A) Hybridization of DNA-AuNP probes with complementary linker strand at 25 °C. (B) Thermal disassembly of DNA-AuNPs at 39.6 °C (T_m + 2). *Experimental conditions:* 60 pmol of linker DNA and 1.5 pmol of both AuNP probes in 1 mL PBS buffer (0.5 M NaCl, 10 mM PBS, 0.01% SDS, pH 7).

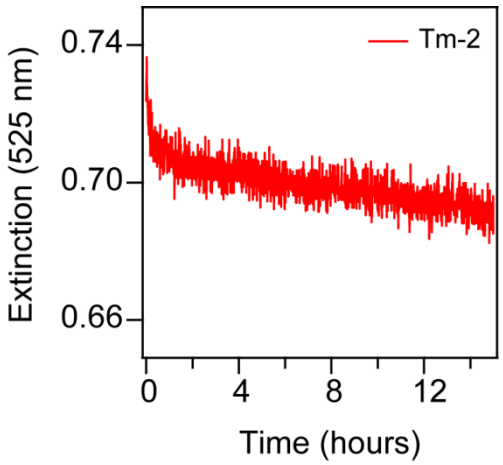

Figure 2.3. Aggregation of DNA-AuNP with linker DNA at T_m – 2 (35.6 °C). The two AuNP probes and linker DNA were combined at time zero. The absorbance change was minimal after 13+ hours indicating that hybridization and aggregation was exceptionally slow at this temperature.

Consistent with previous studies, assembly of these materials by hybridization at room temperature required more than 12 hours for complete aggregation (Figure 2.2A).[81] In contrast, upon heating we were able to disperse these aggregates into colloidal gold in a matter of minutes. Specifically, we monitored dissaggregation by placing an aggregate mixture assembled at room temperature into a temperature-controlled spectrometer set to 39.6 °C (T_m + 2). Dissociation occurred within five minutes of placing the sample into the temperature controller, thereby including the time required to heat the solution and promote dissociation (Figure 2.2B). In contrast, very little hybridization was observed over 15 hours when the two AuNP probes were combined with the complementary linker at higher temperatures revealing that aggregation by hybridization was indeed a slow process (Figure 2.3).

In the strand displacement assay, the target DNA forms a more stable complex with the linker than the original linker-DNA-AuNP aggregate. This difference in stability is observable in the different melting temperatures of the two systems. For example, the aggregates formed from the linker strand and two AuNPs have a T_m of ~36 °C (Figure 2.4) while the calculated T_m of the linker:target duplex is 49 °C under the same experimental conditions.[82]

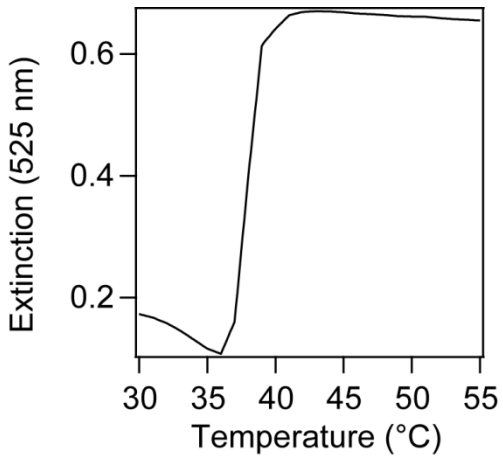

Figure 2.4. (A) The sharp melting (ie. thermal dissociation) transition of duplex-linked aggregates measured with 1 °C increments and a 1-minute hold time at each temperature setting.

This difference in stability is due to the formation of a complete duplex between the linker and the target in contrast to the nicked duplex that forms between the linker and the DNA-AuNPs (Figure 2.1). Our kinetic analysis of formation and disassembly supported our hypothesis that aggregate dissociation by strand displacement should be faster than aggregate association by direct DNA hybridization. However, the previous work by Sturla and co-workers reported that

strand displacement using the strategy shown in Figure 2.1 required multiple hours when performed at room temperature, which was ~6 °C less than the dissociation temperature of the aggregates (T_m = 31.3 °C).[69] We reasoned that displacement in their experiments was slow owing to the slow off rate of the linker-DNA-AuNP complex at room temperature. To determine whether the displacement process could be sped up, we investigated the strand displacement rate as we neared the T_m of the duplex-linked aggregate. The ability to perform assays near the melting temperature without disassembling the aggregates is one advantage of the sharp thermal transitions of these materials (Figure 2.4). Unlike molecular DNA probes, negligible dissociation of the aggregate occurs at a few degrees below the T_m (Figure 2.5).[83]

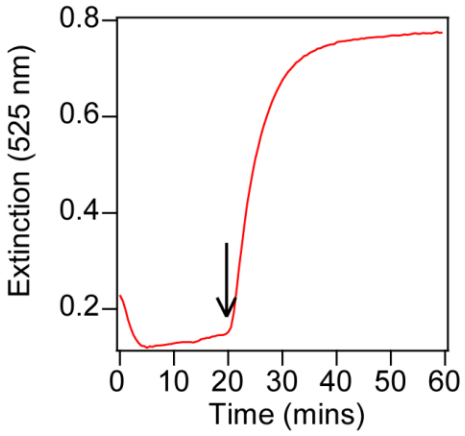

Figure 2.5. The results of a kinetic experiment involving a 20 minute equilibration time to illustrate the negligible dissociation of AuNP aggregates at T_m – 2 (35.6 °C). At 20 minutes target was added (black arrow) and an immediate change in extinction at 525 nm was observed over the next 40 minutes.

2.3.2 Kinetic Experiments: Varying Temperature

Prior to performing target-triggered strand displacement, DNA-AuNPs were first hybridized with linker strands overnight at lab temperature to form aggregates with low extinction values at 525 nm. The aggregates were then incubated for 20 minutes at various temperatures with respect to the aggregate melting temperature: T_m - 2 °C, - 4 °C, - 6 °C and - 8 °C (35.6, 33.6, 31.6, 29.6 °C, respectively). After this wait time, target DNA was added while monitoring the extinction at 525 nm.

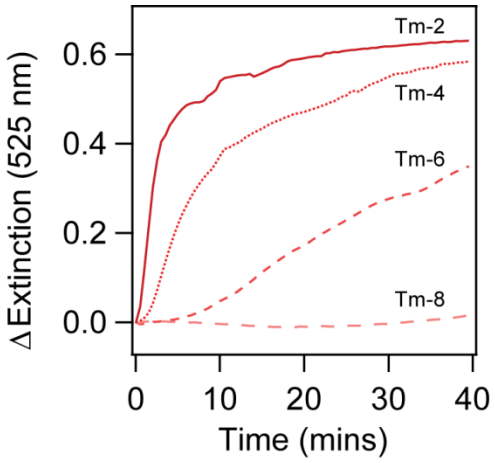

Figure 2.6. Results of monitoring the kinetics of target-triggered strand displacement at four different temperatures (34.8 °C, 32.8 °C, 30.8 °C, 28.8 °C, respectively) with respect to the melting temperature (T_m = 36.8 °C) using 60 pmol (60 nM) target.

As shown in Figure 2.6, when the temperature was 2 °C less than the aggregate T_m, there was a rapid and significant increase in extinction upon the introduction of target, which corresponded to a color change from blue precipitate to red colloid. Target-triggered disassembly at T_m - 4 °C and T_m - 6 °C was also observed based on immediate changes in extinction at 525 nm although at T_m - 6 °C the extent of change

as well as the rate was much slower. In contrast, the system at T_m - 8 °C did not show extinction changes even after 40 minutes indicating that aggregates were still present. These results support that displacement of the linker strand was highly favorable at higher temperatures and very slow at temperatures that were further from the aggregate T_m.

2.3.3 Kinetic and Thermal Denaturation Experiments: Varying Concentration of Target and Varying Concentration of Aggregate

After establishing that the strand displacement assay was very rapid at T_m - 2 °C, we next monitored the effects of changing the amount of target on the response rate of the system. As shown in figure 2.7A, upon adding 30 pmol, 15 pmol or 5 pmol of target strand (corresponding to 30 nM, 15 nM and 5 nM final concentrations, respectively), there was an increase in time required to disassemble the DNA-AuNPs at ~36 °C (T_m - 2 °C). We speculate that the target strands were only able to displace the surface linker strands of the DNA-AuNP aggregates resulting in a slower colorimetric change as well as lower change in extinction. Indeed, when we scaled the system down so that the linker concentration was equal to the target concentration for these lesser amounts of target, we observed rapid dissociation with 15 – 60 pmol target (Figure 2.7B). However, by scaling down the amount of linker and AuNP-DNA we were unable to observe the presence of 5 pmol of target (5 nM) in contrast to the experiment using excess linker and AuNPs.

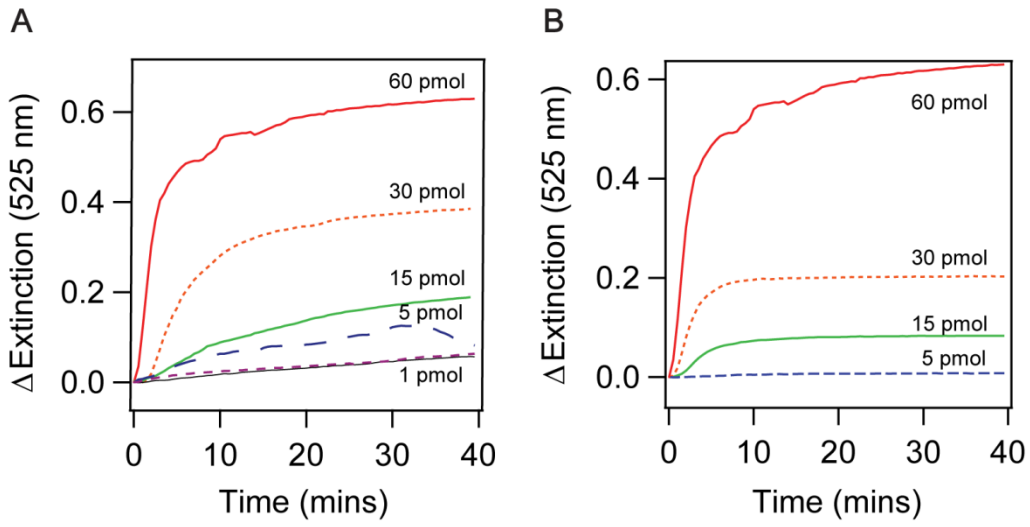

Figure 2.7. Kinetic analysis of strand displacement at T_m - 2 °C (A) as a function of added target with constant DNA-AuNP (1.5 nM) and linker (60 nM) concentrations and B) as a function of added target at T_m - 2 °C with decreasing DNA-AuNP and linker concentrations while maintaining the target;DNA-AuNP: linker molar ratio of ~40:1:40.

2.4 Conclusion

In this study we have developed a system that is rapidly able to detect ssDNA using colorimetric read-out quantified by UV-vis absorbance spectroscopy. By going against the conventional wisdom of using aggregation based assays in colorimetric detection, which require long wait times, we were successful at generating the reverse whereby introduction of the target at a precise temperature triggers disaggregation. Specifically, by monitoring the effect of temperature on the displacement reaction of our DNA-AuNP aggregates, we found that at T_m - 2 we observed rapid strand displacement compared to T_m – 10, where displacement occurred over a long period

of time. In addition, we found that target displacement in the presence of lower amount of target exhibited increased change in extinction compared to scaling down the amount of linker:DNA-AuNP:target. To conclude, by exploiting the sharp melting transition of these DNA-AuNP aggregates and through systematic design, we were able to develop a rapid colorimetric detection assay providing read out of 10 pmol of DNA in less than 10 minutes. Despite the capabilities of this rapid colorimetric system, there are potential drawbacks, namely that the melting temperature must be known beforehand and also the narrow temperature window at which this assay must be performed. The following chapter will further address these issues.

Chapter 3: Tuning Toehold Length and Temperature to Achieve Rapid, Colorimetric Detection of DNA from the Disassembly of DNA-Gold Nanoparticle Aggregates

3.1 Introduction

Since the advent of DNA-modified gold nanoparticles in the mid 1990's the ability to program the function of gold nanoparticles has been revolutionary.[59,84] The fabrication of an inorganic metal colloid with organic components has offered tremendous possibilities in many practical applications such as biodiagnostics and therapeutics. However, our focus in this chapter is utilizing DNA functionalized AuNPs and their ability to disassemble in the presence of ssDNA as a colorimetric detection platform.[48] Previous reports have studied aspects associated with ssDNA induced aggregation of DNA-AuNPs, in particular the effect of gaps and overhangs on this linking strand and its impact on aggregate stability and the rate of formation.[68,71] In addition, temperature, salt concentration, pH and the structure of the thiolated moiety on the AuNP-bound strands have also been explored.[50,85-87] Although many studies have demonstrated the feasibility of aggregating AuNP as a colorimetric method in biodetection, these methods remain relatively slow requiring hours for complete aggregation.[68,78] Moreover, the reverse system utilizing disassembly of aggregates has also been demonstrated in various studies, yet still remains quite slow at room temperature.[38,69] Therefore one question remains: how does the temperature affect the detection rate of these aggregates in the presence of its respective target DNA strand? As mentioned in the previous chapter, one less desirable feature of the

rapid target-triggered disaggregation approach using strand displacement is the need to know the T_m of the system in advance and to perform the assay at a temperature that is near the melting temperature (T_m – 2). One potential solution to increase the temperature range where strand displacement is rapid is to have the linker contain bases that are unhybridized in addition to those bases hybridized to the AuNP probes (also known as a toehold). This single-stranded region facilitates preferential displacement through the introduction of the ssDNA target that is fully complementary to both the hybridized and unhybridized regions of this linker strand (Figure 3.1).[88,89]

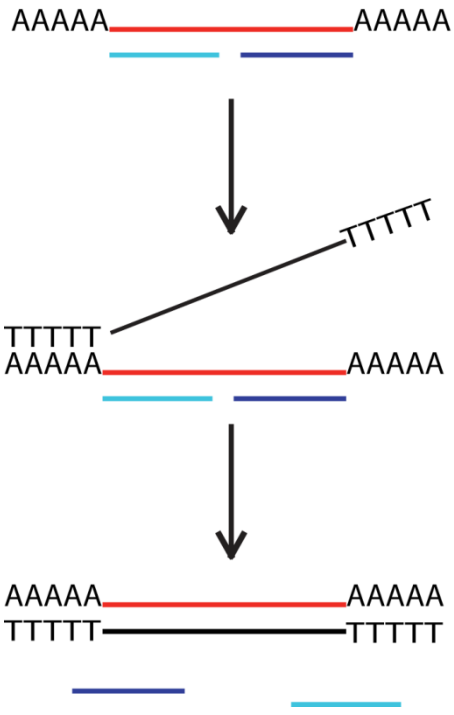

Figure 3.1. A schematic illustrating toehold mediated strand displacement. Single-stranded polydeoxyadenosine regions (toeholds) terminate each end of a three-strand

duplex. The introduction of a target strand that is also complementary with the overhang and unzips the duplex displacing the two complementary strands. The driving force is an increase in complementary interactions between the new incoming strand and the toe-hold containing strand.

Toehold mediated strand displacement of AuNPs has been exploited for many reasons, one being the favorable thermodynamic stability associated with increased base pairing.[89] Hazarika et al. demonstrated the reversibility of AuNP aggregation using DNA fuel strands, based on the repeated additions of linker strands that fuel aggregation and target strands that fuel disaggregation via toehold mediated strand displacement.[48] Duan et al. has also utilized toeholds in a cascade that ultimately displaces DNA-AuNP aggregates in a colorimetric detection system.[90] In addition, toehold mediated systems have been used for colorimetric AuNP aggregation in a logic gate system using DNA-AuNP hybridization for potential use in multiplexing.[91] More interestingly, displacement strategies utilizing gaps and linkers tethering complementary AuNP probes have been examined with respect to colorimetric output.[38,90,92] For example, in a recent study showing target induced AuNP aggregate disassembly was demonstrated with a 50% disassembly in just over 20 minutes and almost 100% disassembly in an hour.[68] However, one aspect of these systems that has not been yet examined is the effect of both toehold length and temperature on the rate of target-triggered disaggregation. Here we demonstrate how target induced disassembly can be rapidly achieved in 10 minutes or less allowing for simple colorimetric detection of DNA down to low concentrations (5 nM; 5 pmol/mL) by

carefully tuning the assay temperature window to facilitate rapid strand displacement. By using the optimal length toehold, detection is possible over a wide temperature range, including room temperature, allowing for visual detection of 10 pmol target DNA in 10 minutes. In addition to demonstrating the feasibility of DNA-AuNP aggregate disassembly at room temperature, we provide a novel approach to making this assay suitable for long-term storage based on the lyophilization of DNA-AuNP aggregates. We monitored the assay performance as a function of solid phase storage temperature (of the lyophilized aggregates) to determine the robustness of the system in a POC application.

3.2 Experimental

3.2.1 DNA Syntheses and Characterizations

All reagents were purchased from Glen Research to synthesize DNA strands by solid-phase synthesis. Solid-phase synthesis was performed on an Applied Biosystems Model 392 DNA/RNA Synthesizer. Concentration calculations were conducted on an HP 8453 diode-array spectrophotometer equipped with a HP 89090A Peltier temperature controller. All DNA concentrations were determined from their absorbance at λ = 260 nm and extinction coefficients determined by Oligocalc.[79] Additionally, all samples, buffers, solutions were dissolved in MilliQ water (18.1ΩM)

Following DNA synthesis, samples were either deprotected overnight with 1 mL NH_4OH at room temperature or quickly deprotected with 1 mL NH_4OH at 65°C for 2 hours. The strands were then purified using a DMT-On procedure with Glen-Pak Cartridges (Glen Research, Catalogue # 60-5200-01). All bases used to synthesize

DNA were standard nucleotide phosphoramidites. Additionally, Thiol-Modifier C6 (10-1936-90) and 3' Thiol-Modifier C3 S-S controlled porous glass (CPG) (Catalogue # 20-2933-41) were used to synthesize thiolated strands. Purified DNA was lyophilized before placing in the freezer for future use.

Table 2.1. DNA sequences and modifications

Probes	**DNA Sequences and Modifications**
Probe A:	5'- S-C6* AAA AAA AAA ATT GTT AAA T -3'
Probe B:	5'- ATT GAT AAG AAA AAA AAA A *C3-S -3'
OA_1:	5'- ACT TAT CAA TAT TTA ACA AA -3'
OA_3	5'- AAA CTT ATC AAT ATT TAA CAA AAA -3'
OA_5	5'- AAA AAC TTA TCA ATA TTT AAC AAA AAA A -3'
OA_7	5'- AAA AAA ACT TAT CAA TAT TTA ACA AAA AAA AA -3'
OA_9	5'- AAA AAA AAA CTT ATC AAT ATT TAA CAA AAA AAA AAA -3'
OT_1	5'- TTT GTT AAA TAT TGA TAA GT -3'
OT_3	5'- TTT TTG TTA AAT ATT GAT AAG TTT -3'
OT_5	5'- TTT TTT TGT TAA ATA TTG ATA AGT TTT T -3'
OT_7	5'- TTT TTT TTT GTT AAA TAT TGA TAA GTT TTT TT -3'
OT_9	5'-TTT TTT TTT TTG TTA AAT ATT GAT AAG TTT TTT TTT-3'

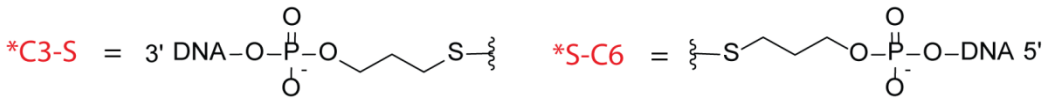

3.2.2 Gold Nanoparticle Synthesis

Gold nanoparticles with 13 nm diameter were synthesized as per previous reports.[8,9,64] The details of the procedure are provided in Chapter 2 (Section 2.2.2).

3.2.3 DNA Loading on Gold Nanoparticles

The loading of thiolated DNA to gold nanoparticles followed the procedure of Hurst et al. with a few modifications.[50] The details of the procedure are provided in Chapter 2 (Section 2.2.3). The only changes are that during salt aging, the sample mixtures are salted up to 0.7 M NaCl compared to 0.5 M NaCl in the previous chapter using a 2 M NaCl buffer (2 M NaCl, 10 mM PBS, 0.01% SDS, 0.5% NaN_3, pH 7).

3.2.4 Purification and Hybridization of Gold Nanoparticles

After two days (or more) of incubation of the DNA-AuNP after reaching the highest salt concentration (0.7 NaCl), the purification of these AuNP probes were performed as outlined by Hurst et al. with slight modification.[50] The details of the procedure are provided in Chapter 2 (Section 2.2.4). The only change made was that the buffer used for purification was changed to 0.7 M NaCl (0.7 M NaCl, 10 mM PBS, 0.01% SDS, 0.5% NaN_3, pH 7) from 0.5 M NaCl.

3.2.5 Kinetic and Thermal Denaturation Experiments

Kinetic experiments were conducted with the hybridization mixture as stated in the procedure in Chapter 2 (Section 2.2.4). Detailed procedure regarding kinetic and

thermal denaturation experiments are provided previously in Chapter 2 (Section 2.2.5)

3.2.6 Lyophilization of DNA-AuNP Aggregates

Pre-formed aggregates (1 mL) in 1.6 mL eppendorfs presented above in Section 3.2.4 were allowed to hybridize for 1 day or more before they were tabletop centrifuged for 10 seconds to form a small pellet. Then, 900 μL of the supernatant was decanted and discarded, and the remainder was frozen in dry ice for approximately 5 minutes. The eppendorf sample was placed on a lyophilizer for greater than 24 hours to yield lyophilized aggregates.

3.2.7 Temperature Storage Experiments with Lyophilized DNA-AuNP Aggregates

Lyophilized samples of the DNA-AuNPs were stored at varying temperatures of -20 °C, 4°C, 22 °C (RT), and 40 °C for two weeks. After two weeks, each sample was reconstituted with MQ H_2O (100 μL) and then lightly vortexed and table top centrifuged. These samples were allowed to sit at room temperature for approximately 10 minutes before adding 60 pmol of target DNA (in 5 μL) into each of the samples. Control experiments were also performed where instead of target addition, 5 μL of 0.7 M NaCl buffer was added. Immediately after sample addition, samples were shaken and monitored for 15 minutes, pictures were taken at 5 minute and 10 minute intervals. Duplicate experiments were performed at each temperature storage setting.

3.3 Results and Discussion

3.3.1 Design of Temperature-Insensitive Assay using Toehold Mediated Strand Displacement

As mentioned in the previous chapter, one disadvantage of direct target-triggered strand displacement is that the melting temperature T_m must be known beforehand. More importantly, the visualization assay using target-triggered strand displacement without toeholds is confined to a narrow operational temperature window near the T_m. To eliminate this requirement, the system needed to be redesigned in such a way that rapid disassembly occurred over a broader range of temperatures below the T_m. A wide range of operational temperatures would also allow this method to be applicable at room temperature, circumventing the need for heating equipment, which is desirable for point-of-care assays.[21,93,94] To accomplish this goal, we explored the effect of modifying both ends of the linker DNA strands with differing lengths of overhangs, nucleotide extensions that do not participate in hybridization with the probe strands. The target strand is modified similarly in order to be fully complementary to the extended linker, leading to aggregate disassembly that occurs via a toehold mediated strand displacement mechanism (Figure 3.2).

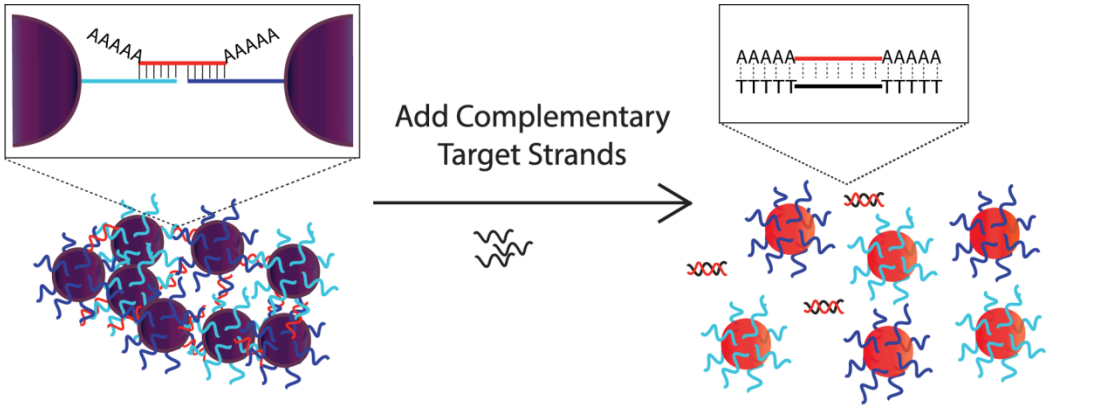

Linker Strands

oA1: 5'-ACTT ATC AAT ATT TAA CAAA-3'

oA3: 5'-AAACTT ATC AAT ATT TAA CAAAAA-3'

oA5: 5'-AAAAACTT ATC AAT ATT TAA CAAAAAAA-3'

oA7: 5'-AAAAAAACTT ATC AAT ATT TAA CAAAAAAAAA-3'

oA9: 5'-AAAAAAAAACTT ATC AAT ATT TAA CAAAAAAAAAAA-3'

Target Strands

oT1: 5'-TTTG TTA AAT ATT GAT AAGT-3'

oT3: 5'-TTTTTG TTA AAT ATT GAT AAGTTT-3'

oT5: 5'-TTTTTTTG TTA AAT ATT GAT AAGTTTTT-3'

oT7: 5'-TTTTTTTTG TTA AAT ATT GAT AAGTTTTTTT-3'

oT9: 5'-TTTTTTTTTTG TTA AAT ATT GAT AAGTTTTTTTTT-3'

Figure 3.2. Scheme illustrating linkers with varying polyadenosine overhang (toehold) lengths used to aggregate AuNP probes, followed by toehold mediated strand disassembly with target DNA.

3.3.2 Thermal Stability of Aggregates as a Function of Overhang (Toehold) Length

To determine the influence of toehold length on the stability of the resulting aggregate, we formed a series of aggregates containing polydeoxyadenosine overhangs on both ends of the linker strand (OA_X, where x is the number of adenosine units on each end). Consistent with previous reports, we found that increasing the strand length of the linker strand led to a decreased T_m (Figure 2.3), which can be attributed to steric destabilization of the aggregate owing to the presence of the overhangs.[57,71] Additionally, the overall change in extinction

decreased as a result of the formation of smaller aggregates, which became more pronounced with increasing overhang length.

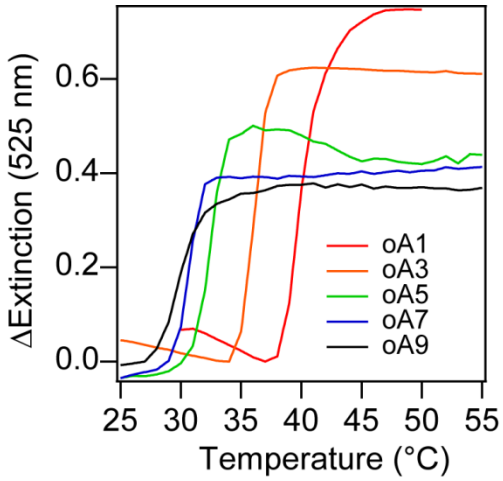

Figure 3.3. Melting curve of aggregates composed of linkers with varying overhang lengths.

3.3.3 Kinetics of Target-triggered Aggregate Disassembly as a Function of Overhang Length and Temperature

To determine if these overhangs could act as toeholds for strand displacement, we added the corresponding complementary target for a range of temperatures below the T_m of the given aggregate system ranging from $T_m - 2$ to $T_m - 10$ (Figure 3.4). We observed that changing the length of the toehold domain resulted in systematic changes in the temperature window at which rapid strand displacement occurred upon addition of the target strand. For example, if we evaluate the extent of dissociation after 10 minutes, we observed that as the overhang length increased to 5 bases, the temperature range over which we witnessed rapid dissociation widened: at least 50% of OA_5 aggregates dissociated within 10 minutes even at $T_m - 10$, equating to an

operational temperature range of 22.5 °C to 30.5 °C. As we increased the overhang length to 7 and 9 bases, we observed that this temperature window decreased somewhat due to the T_m systematically decreasing. Thus, the optimal overhang length is between 5 and 7, which is approximately half of the length of the polydeoxyadenosine spacer of the probe DNA. This length corresponds to the length just before steric effects start to negatively affect target binding.[91] By understanding how altering the overhang length influences both the T_m as well as the operational temperature range for rapid disaggregation, assay for different targets can be rationally designed.

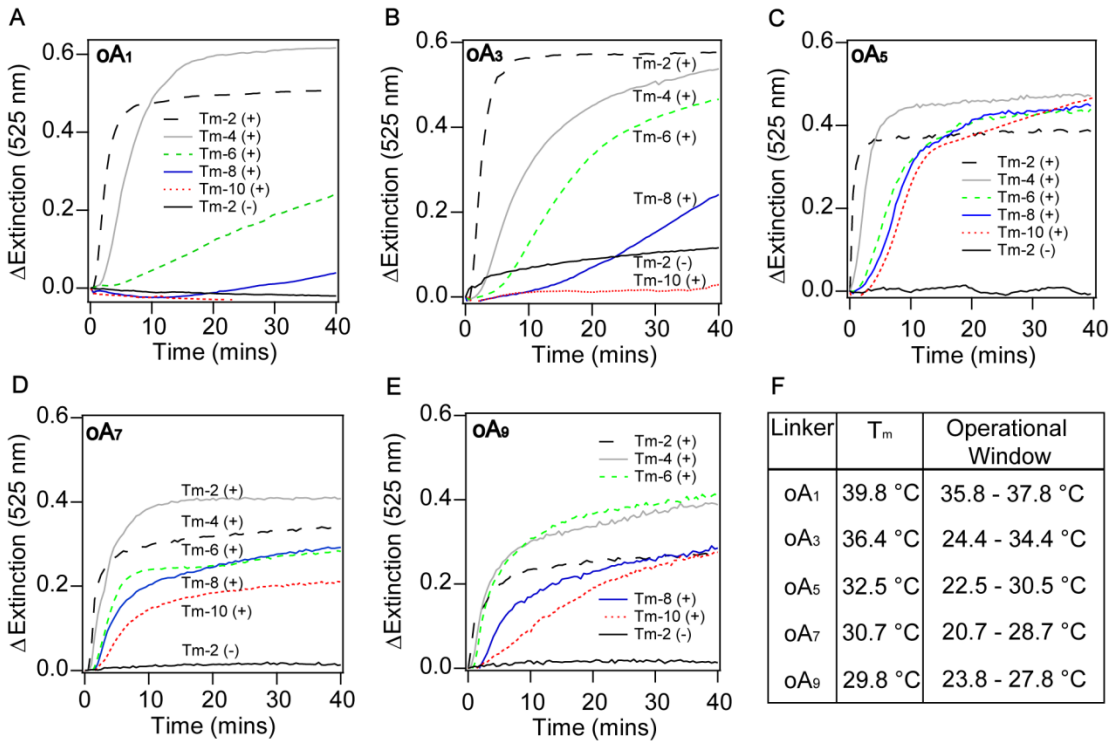

F

Linker	T_m	Operational Window
oA_1	39.8 °C	35.8 - 37.8 °C
oA_3	36.4 °C	24.4 - 34.4 °C
oA_5	32.5 °C	22.5 - 30.5 °C
oA_7	30.7 °C	20.7 - 28.7 °C
oA_9	29.8 °C	23.8 - 27.8 °C

Figure 3.4. (A) to (E) Kinetics of target-triggered strand displacement at temperatures below the T_m of each set of aggregates, for linkers with overhangs of 1, 3, 5, 7, and 9 bases, respectively. Each set was run with premade aggregates of 1.5 pmol of each AuNP probe A and AuNP probe B and 60 pmol of overhang linker strand. After a 20 minute equilibration period, 60 pmol of target complementary to the linker was added (+). For the control (-), buffer without target was added. (F) Melting temperatures and operational temperature windows of the various toehold mediated strand displacement assays.

3.3.4 Direct Visualization of Target-triggered Aggregate Disassembly

The previous experiments utilized UV-vis absorbance spectroscopy to monitor aggregate disassembly, but the ideal system should be colorimetric (ie. visible to the

naked eye). To determine the efficacy of the system as a colorimetric assay, aggregates were formed from 150 fmol of each AuNP probe and 6 pmol of linker strand OA_5 combined in 20 µL of 0.7 M NaCl buffer and left overnight (or longer) at room temperature. Varying amounts of target DNA, 0 – 100 pmol in 20 µL, were then added to separate samples. The mixtures were immediately shaken, and pictures were taken after 10 minutes of standing (Figure 5). As can be seen in the image, as little as 10 pmol of DNA can be detected rapidly by the naked eye in this room temperature assay.

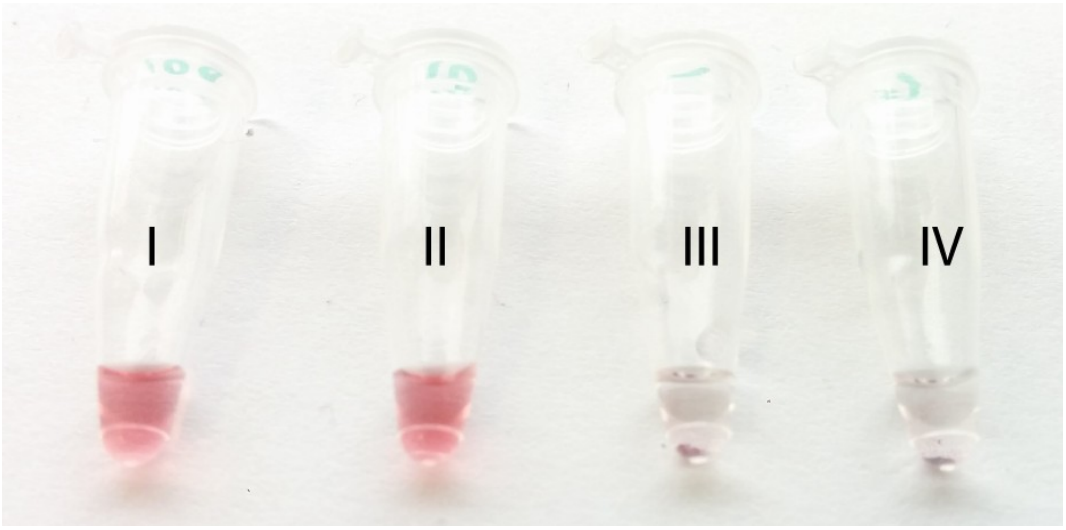

Figure 3.5. Target (OT_5) added to DNA-AuNP (150 fmol) and linker (OA_5, 6 pmol). Target amounts used were i) 100 pmol, ii) 10 pmol, iii) 1 pmol, iv) no target.

3.3.5 Influence of Aggregate Lyophilization and Storage Temperature on the Target-triggered Aggregate Disassembly Assay

In an effort to further demonstrate the robustness of our assay, we took AuNP aggregate samples made from linkers containing 5-base overhangs (OA_5) and lyophilized them after decanting 900 µL of buffer from the sample. Our intention of

performing these experiments was to test the functionality of our DNA-AuNP aggregates mimicking storage conditions encountered around the world. Consequently, solid phase aggregates were stored in varying temperature conditions of -20 °C to 40 °C for two weeks.

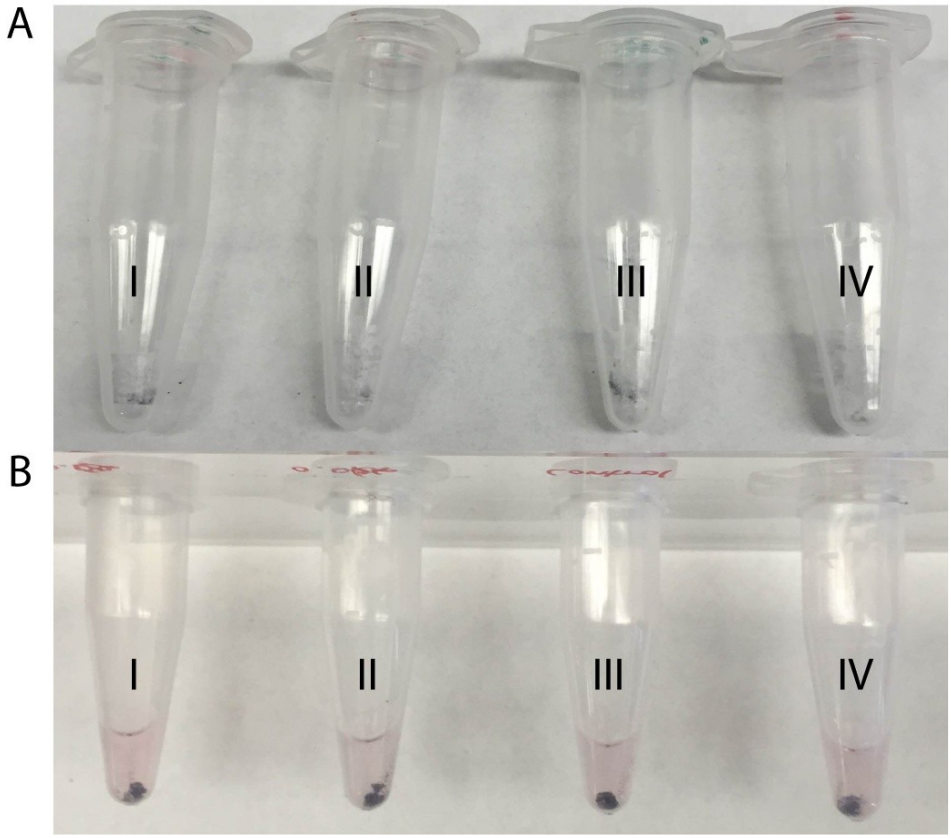

Figure 3.6. (A) Lyophilized DNA-AuNP aggregates (I to IV) after storage at various temperature conditions of -20 °C, 4 °C, 22 °C (Lab Temp), 40 °C for two weeks. (B) Reconstituted DNA-AuNP aggregates (I to IV) with various temperature conditions, as per above, with 100 µL of H_2O.

Upon lyophilization, we observed a significant color change (Figure 3.6A) and reasoned that the mechanical and temperature stress associated with lyophilization and storage would not allow these samples to be disassembled, similar

to what has been observed for lyophilized citrate-stabilized AuNPs.[95] However, upon reconstitution with H_2O (100 µL), our solution was an off purple color indicating that some of the DNA-modified AuNPs were intact (Figure 3.6B).

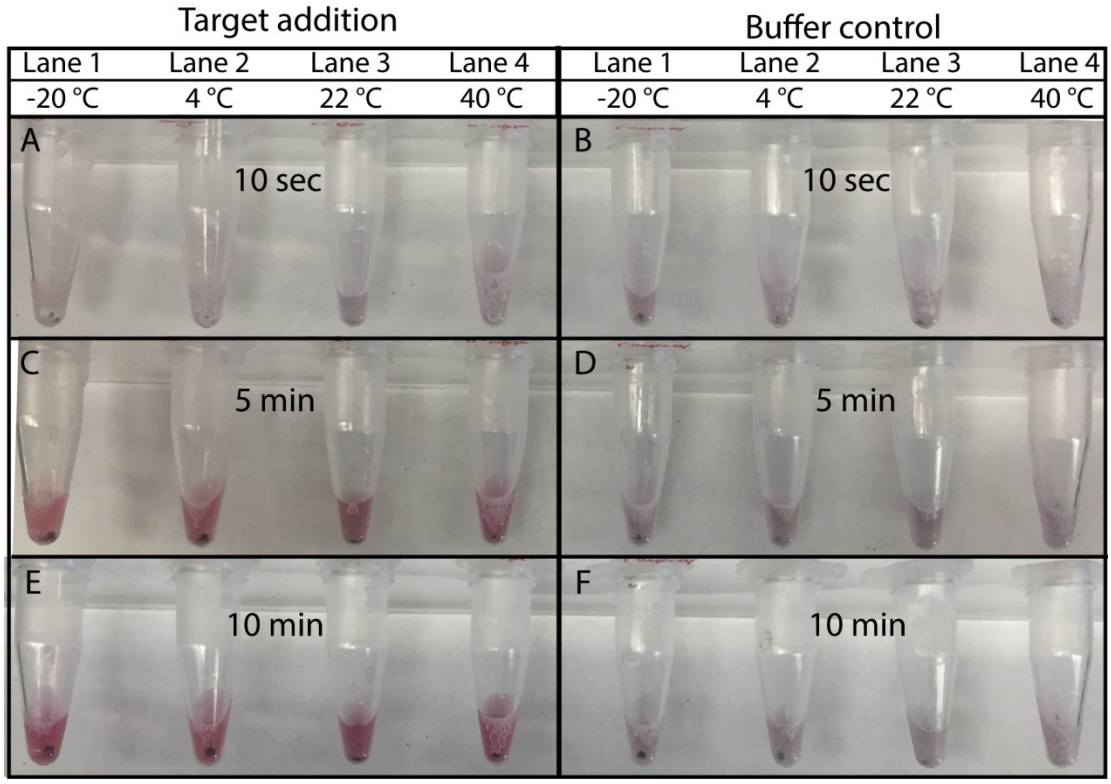

Figure 3.7. Lyophilized DNA-AuNP aggregates stored for two weeks at various temperatures (Lanes 1 to 4: -20 °C, 4 °C, 22 °C, 40 °C respectively) before reconstitution with H_2O (100 µL), afterwards, target addition (60 pmol, 5 µL) compared with 0.7 M NaCl buffer (5 µL) controls are illustrated for each temperature storage condition. (A) Pictures of samples with target addition compared with (B) illustrating buffer addition without target, pictures are taken immediately after hand shaking samples. (C) and (E) are pictures taken at 5 and 10 minute intervals following target addition, whereas, (D) and (F) are the buffer control comparisons also at 5 and 10 minute intervals.

What was more interesting was that after target addition (60 pmol, OT_5) and light shaking by hand, disassembly occurred after 5 minutes based on the emergence of a faint red color (Figure 3.7). Moreover, the storage temperature of the lyophilized sample had a minimal effect on this strand displacement. As the color increased after a further 10 minutes, we observed that all samples were indeed disassembling at room temperature. In addition, after 15 to 20 minutes, the distinction between aggregates with and with target was very significant (Figure 3.8). We concluded that lyophilization preserved the recognition ability of the aggregated AuNPs linked through DNA hybridization.

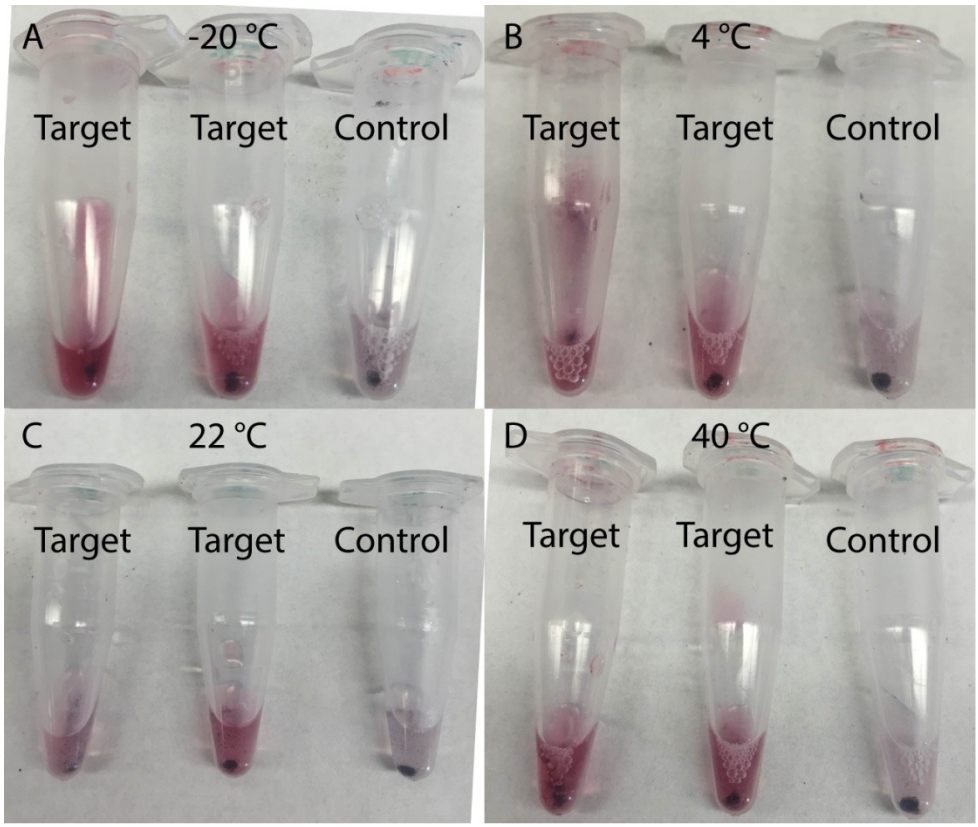

Figure 3.8. Reconstituted DNA-AuNP aggregates that have had target added (left and middle) and buffer control (right) in (A) to (D) with various temperature storage conditions of -20 °C, 4 °C, 22 °C and 40 °C respectively. Pictures are taken approximately 15 to 20 minutes after target addition.

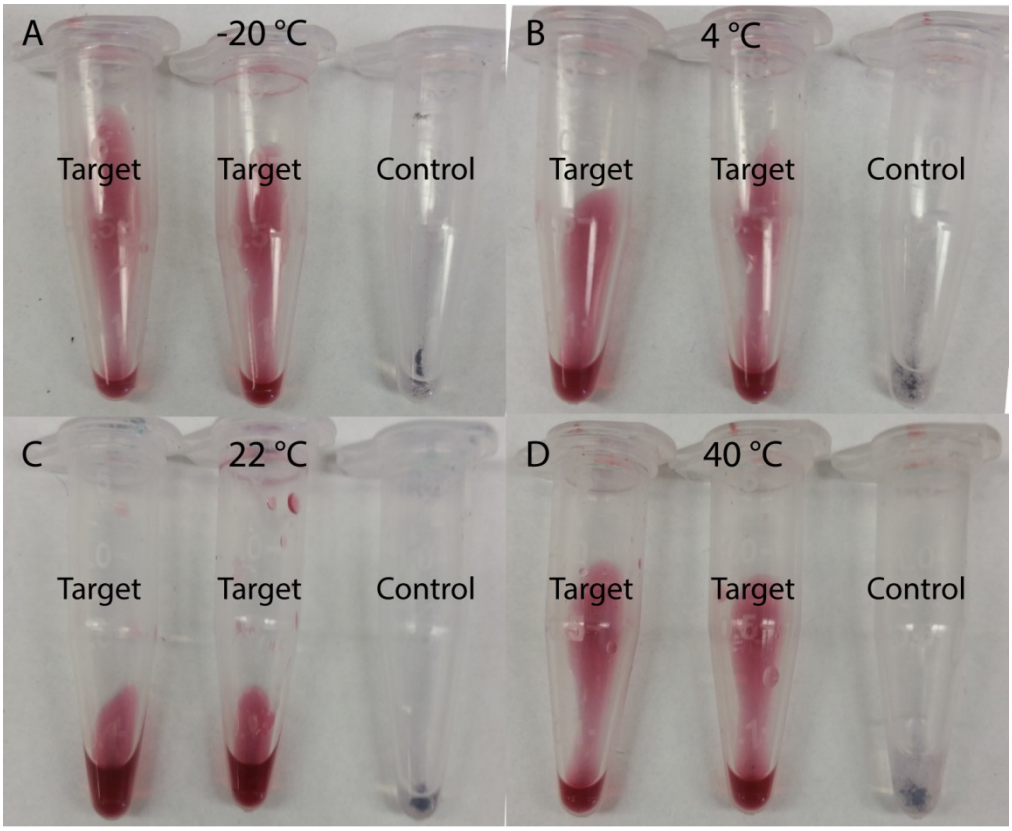

Figure 3.9. Reconstituted DNA-AuNP aggregates that have had target added (left and middle, 60 pmol, 5 µL) and buffer control (no target, right, 5 µL) in (A) through (D) with various temperature storage conditions of -20 °C, 4 °C, 22 °C and 40 °C respectively. Pictures are taken approximately 48 hours after target addition.

One interesting feature of this system was that after extended periods of time (3 days), we irrevocably obtained a permanent, dark ruby red, colorimetric response illustrating that in the presence of target compared to our control (buffer) counterpart which was still in an aggregated state as illustrated in Figure 3.9. In addition, when we closely examine aggregate sample 10 minutes after target addition (Figure 3.8) and two days after target addition (Figure 3.9), we observed full dissolution of the

aggregates in the latter. Whereas in the buffer control, no dissociation was observed even after extended periods of time. These results confirm that lyophilized DNA-AuNP aggregates completely retain their ability to undergo toehold mediated strand displacement increasing their potential for POC applications.

3.4 Conclusion

In this chapter, we have shown that by increasing the toehold length of our linker strand and hybridizing them to AuNP probes, we can effectively alter the temperature window at which we obtain colorimetric detection. We demonstrated that when we increased the overhang length to approximately 5 and 7 bases (OA_5 and OA_7) on each end, we can effectively run the assay at temperatures 10 °C below the T_m. However, when we have an overhang length that is close to the spacer length (OA_9) and displace it with complementary target, the disassembly process was slower which can be attributed to steric hindrance. By using the optimal overhang length of 5 bases on each end, we observed a colorimetric response at room temperature upon adding target in a bench top liquid assay. Finally, by lyophilizing our DNA-AuNP aggregates, we demonstrated the robustness of our system to various storage temperatures, which is an important consideration for point-of-care diagnostics. This work establishes that target-triggered aggregate disassembly is suitable as a bench top colorimetric detection method and is amenable to long-term storage even at elevated temperatures.

Chapter 4 – Concluding Remarks and Future Work

This thesis has highlighted some important advances in understanding the linker to AuNP probe dependence of temperature associated with the colorimetric disassembly of AuNP aggregates. Not only is temperature a factor in determining the amount of dissociation, but by increasing the amount of overhangs to approximately half the spacer length, it is demonstrated that the temperature window in this assay is indeed a critical parameter that can be tunable in design. Our initial goal at the beginning of the project was to initially develop a point of care kit which is still an ongoing venture. Although this thesis is no means comprehensive of the parameters explored, it does provide insight towards designing and synthesizing a DNA-AuNP colorimetric disassembly system that takes into consideration not only the steric effects of the overhang length but also the temperature range determined by the T_m of the system. By applying these guidelines and work from previous reports studying other important parameters,[50,68,70,71] I believe that this work has potential to be used in optimizing existing or novel systems with respect to colorimetric disassembly. Many previous reports have addressed single nucleotide polymorphisms (SNP) as a potential problem in mutations and have long since elucidated many of the underlying parameters in determining a perfect DNA match.[2,64,69] Whereas others have developed methodologies involving lateral flow assays (LFAs) that detect small analytes using aptamer functionalized AuNPs.[38,56] Despite AuNPs being a simple, robust and easy to use colorimetric system, one major drawback still involves the DNA assay turnaround time to sensitivity such as reports demonstrating catalytic systems which remain quite slow despite their modest sensitivity. [69,91]

Within every system, there is always a tradeoff, and colorimetric detection being quick, easy to use and robust, makes it the most viable choice for consumers who may not necessarily have access to sophisticated instrumentation.[77] The future directions in which we intend to strive towards is one in which we tackle the problem of versatility while balancing the speed and sensitivity of our assay in the storage of our DNA-AuNP aggregate assay ultimately mitigating the risk for solution phase changes that could occur over months to years. Shelf life is an important parameter in the pharmaceutical industry, where lyophilization is often employed to extend the storage of drugs, vaccines and biological materials.[96,97] One great example was shown with silver nanoparticles (AgNPs), where they were able to effectively create a powder and successfully re-suspend the AgNPs in a reproducible monodisperse manner.[98] Many studies have already shown the conjugation of cancer drugs such as doxorubicin onto the surface of AuNPs and the ability to selectively target cancerous cells.[99] Lyophilization is one factor that would largely benefit any therapeutic application that could potentially be used in drug delivery or drug design as it extends the storage capabilities of these materials.

One interesting proposal which is still in the process of optimization is developing a system in which we our system in which AuNP aggregates are freeze dried or immobilized in a solid state whereupon we introduce a target to illicit a colorimetric response. As mentioned previously, Liu and coworkers were able to effectively create a system using "size exclusion" on the LFA. By utilizing the same format, a creative design can be made where the addition of target should be able to elicit a colorimetric response using disassembly.[56] Although our group only briefly

looked at the applications of this system, it has proven to be a worthwhile venture. We have been able to effectively lyophilize AuNPs aggregates and preliminarily created a solid phase means for portability and storage. Although preliminary studies into this idea have brought about significant results as discussed in Chapter 3, there are still many parameters to be explored. One potential concern is that we are still unable to determine the phenomenon of is the broad melting curve exhibited by these lyophilized AuNP aggregates. One speculation regarding the nature of the melting curves is that during the freezing process, fusion and coalescence could potentially disrupt the structural integrity of the DNA-AuNPs, thus leading to this phenomenon.[100] Another form of concern is associated with the integrity of the thiolated DNA strands due to concentrated salt conditions during the freezing process and the removal of hydrogen bonding interactions from water molecules causing linker strands that could potentially be damaged or unbound in these aggregate systems which disrupts the cooperative melting behavior before lyophilization exhibited in many previous works.[60-63,101] One solution to this problem mentioned in a previous report with regards to coalescence and fusion was adding various mono and disaccharides, in particular sucrose, as a cryoprotectant into the buffer solution allowing continual reversible colloidal AuNP freeze-thaw trials.[95,100] Despite our current modest colorimetric detection limit of 60 pmol target in less than 10 minutes at temperatures varying from -20 °C to 40 °C, we believe that by optimizing this system we could potentially achieve high femtomol to low picomol detection limits as well as obtain a readout in less than 5 minutes and possibly creating an applicable POC kit. With the use of more carefully crafted designs and further improved

optimizations, the future of nano-materials can not only provide insightful applications, but must be continued to eclipse and exceed current competing colorimetric platforms in DNA detection.

Bibliography

(1) Dykman, L. A.; Khlebtsov, N. G. Gold nanoparticles in biology and medicine: Recent advances and prospects. *Acta Naturae* **2011**, *3*, 34-55.

(2) Rosi, N. L.; Mirkin, C. A. Nanostructures in biodiagnostics. *Chem. Rev.* **2005**, *105*, 1547-1562.

(3) Yguerabide, J.; Yguerabide, E. E. Light-scattering submicroscopic particles as highly fluorescent analogs and their use as tracer labels in clinical and biological applications - II. Experimental characterization. *Anal. Biochem.* **1998**, *262*, 157-176.

(4) Eustis, S.; El-Sayed, M. A. Why gold nanoparticles are more precious than pretty gold: Noble metal surface plasmon resonance and its enhancement of the radiative and nonradiative properties of nanocrystals of different shapes. *Chem. Soc. Rev.* **2006**, *35*, 209-217.

(5) Jain, P. K.; Lee, K. S.; El-Sayed, I. H.; El-Sayed, M. A. Calculated absorption and scattering properties of gold nanoparticles of different size, shape, and composition: Applications in biological imaging and biomedicine. *J. Phys. Chem. B.* **2006**, *110*, 7238-7248.

(6) Storhoff, J. J.; Lazarides, A. A.; Mucic, R. C.; Mirkin, C. A.; Letsinger, R. L.; Schatz, G. C. What controls the optical properties of DNA-linked gold nanoparticle assemblies? *J. Am. Chem. Soc.* **2000**, *122*, 4640-4650.

(7) Swierczewska, M.; Lee, S.; Chen, X. Y. The design and application of fluorophore-gold nanoparticle activatable probes. *Phys. Chem. Chem. Phys.* **2011**, *13*, 9929-9941.

(8) Enustun, B. V.; Turkevich, J. Coagulation of colloidal gold. *J. Am. Chem. Soc.* **1963**, *85*, 3317-3328.

(9) Kimling, J.; Maier, M.; Okenve, B.; Kotaidis, V.; Ballot, H.; Plech, A. Turkevich method for gold nanoparticle synthesis revisited. *J. Phys. Chem. B.* **2006**, *110*, 15700-15707.

(10) Miranda, A.; Malheiro, E.; Eaton, P.; Carvalho, P. A.; de Castro, B.; Pereira, E. Synthesis of gold nanocubes in aqueous solution with remarkable shape-selectivity. *J. Porphyr. Phthalocya.* **2011**, *15*, 441-448.

(11) Gole, A.; Murphy, C. J. Seed-mediated synthesis of gold nanorods: Role of the size and nature of the seed. *Chem. Mater.* **2004**, *16*, 3633-3640.

(12) Lohse, S. E.; Murphy, C. J. The quest for shape control: A history of gold nanorod synthesis. *Chem. Mater.* **2013**, *25*, 1250-1261.

(13) Pelaz, B.; Grazu, V.; Ibarra, A.; Magen, C.; del Pino, P.; de la Fuente, J. M. Tailoring the synthesis and heating ability of gold nanoprisms for bioapplications. *Langmuir* **2012**, *28*, 8965-8970.

(14) Sau, T. K.; Murphy, C. J. Seeded and non-seeded methods to make metallic nanorods and nanowires in aqueous solution. *Mater. Res. Soc. Symp. P.* **2004**, *789*, 203-212.

(15) Sperling, R. A.; Parak, W. J. Surface modification, functionalization and bioconjugation of colloidal inorganic nanoparticles. *Philos. T. R. Soc. A.* **2010**, *368*, 1333-1383.

(16) Nuzzo, R. G.; Zegarski, B. R.; Dubois, L. H. Fundamental-studies of the chemisorption of organosulfur compounds on Au(111) - Implications for molecular self-Assembly on gold surfaces. *J. Am. Chem. Soc.* **1987**, *109*, 733-740.

(17) Li, Z.; Jin, R. C.; Mirkin, C. A.; Letsinger, R. L. Multiple thiol-anchor capped DNA-gold nanoparticle conjugates. *Nucleic Acids Res.* **2002**, *30*, 1558-1562.

(18) Sun, J. S.; Xianyu, Y. L.; Jiang, X. Y. Point-of-care biochemical assays using gold nanoparticle-implemented microfluidics. *Chem. Soc. Rev.* **2014**, *43*, 6239-6253.

(19) Baptista, P.; Pereira, E.; Eaton, P.; Doria, G.; Miranda, A.; Gomes, I.; Quaresma, P.; Franco, R. Gold nanoparticles for the development of clinical diagnosis methods. *Anal. Bioanal. Chem.* **2008**, *391*, 943-950.

(20) Mabey, D.; Peeling, R. W.; Ustianowski, A.; Perkins, M. D. Diagnostics for the developing world. *Nat. Rev. Microbiol.* **2004**, *2*, 231-240.

(21) Peeling, R. W.; Mabey, D. Point-of-care tests for diagnosing infections in the developing world. *Clin. Microbiol. Infec.* **2010**, *16*, 1062-1069.

(22) Yager, P.; Domingo, G. J.; Gerdes, J. Point-of-care diagnostics for global health. *Annu. Rev. Biomed. Eng.* **2008**, *10*, 107-144.

(23) Singer, J. M.; Plotz, C. M. Latex Fixation Test .1. Application to the serologic diagnosis of rheumatoid arthritis. *Am. J. Med.* **1956**, *21*, 888-892.

(24) Hu, J.; Wang, S. Q.; Wang, L.; Li, F.; Pingguan-Murphy, B.; Lu, T. J.; Xu, F. Advances in paper-based point-of-care diagnostics. *Biosens. Bioelectron.* **2014**, *54*, 585-597.

(25) Chen, A. L.; Yang, S. M. Replacing antibodies with aptamers in lateral flow immunoassay. *Biosens. Bioelectron.* **2015**, *71*, 230-242.

(26) Peeling, R. W.; Holmes, K. K.; Mabey, D.; Ronald, A. Rapid tests for sexually transmitted infections (STIs): the way forward. *Sex. Transm. Infect.* **2006**, *82*, V1-V6.

(27) Lie, P. C.; Liu, J.; Fang, Z. Y.; Dun, B. Y.; Zeng, L. W. A lateral flow biosensor for detection of nucleic acids with high sensitivity and selectivity. *Chem. Commun.* **2012**, *48*, 236-238.

(28) Yan, L.; Zhou, J.; Zheng, Y.; Gamson, A. S.; Roembke, B. T.; Nakayama, S.; Sintim, H. O. Isothermal amplified detection of DNA and RNA. *Mol. Biosyst.* **2014**, *10*, 970-1003.

(29) Xiao, Z.; Lie, P. C.; Fang, Z. Y.; Yu, L. X.; Chen, J. H.; Liu, J.; Ge, C. C.; Zhou, X. M.; Zeng, L. W. A lateral flow biosensor for detection of single nucleotide polymorphism by circular strand displacement reaction. *Chem. Commun.* **2012**, *48*, 8547-8549.

(30) Hu, J.; Wang, L.; Li, F.; Han, Y. L.; Lin, M.; Lu, T. J.; Xu, F. Oligonucleotide-linked gold nanoparticle aggregates for enhanced sensitivity in lateral flow assays. *Lab Chip* **2013**, *13*, 4352-4357.

(31) Cordray, M. S.; Richards-Kortum, R. R. Review: Emerging nucleic acid based tests for point-of-care detection of Malaria. *Am. J. Trop. Med. Hyg.* **2012**, *87*, 223-230.

(32) Engvall, E.; Perlmann, P. Enzyme-linked immunosorbent Assay (ELISA) quantitative assay of immunoglobulin-G. *Immunochemistry* **1971**, *8*, 871-874.

(33) Boisselier, E.; Astruc, D. Gold nanoparticles in nanomedicine: preparations, imaging, diagnostics, therapies and toxicity. *Chem. Soc. Rev.* **2009**, *38*, 1759-1782.

(34) Hirsch, L. R.; Jackson, J. B.; Lee, A.; Halas, N. J.; West, J. A whole blood immunoassay using gold nanoshells. *Anal. Chem.* **2003**, *75*, 2377-2381.

(35) Kim, W.-J.; Cho, H. Y.; Kim, B. K.; Huh, C.; Chung, K. H.; Ahn, C.-G.; Kim, Y. J.; Kim, A. Highly sensitive detection of cardiac troponin I in human serum using gold nanoparticle-based enhanced sandwich immunoassay. *Sensors and Actuators B: Chemical* **2015**, *221*, 537-543.

(36) Tuerk, C.; Gold, L. Systematic evolution of ligands by exponential enrichment - RNA ligands to bacteriophage-T4 DNA-polymerase. *Science* **1990**, *249*, 505-510.

(37) Lu, Y.; Liu, J. W. Functional DNA nanotechnology: emerging applications of DNAzymes and aptamers. *Curr. Opin. Biotech.* **2006**, *17*, 580-588.

(38) Liu, J. W.; Cao, Z. H.; Lu, Y. Functional nucleic acid sensors. *Chem. Rev.* **2009**, *109*, 1948-1998.

(39) Cekan, P.; Jonsson, E. O.; Sigurdsson, S. T. Folding of the cocaine aptamer studied by EPR and fluorescence spectroscopies using the bifunctional spectroscopic probe C. *Nucleic Acids Res.* **2009**, *37*, 3990-3995.

(40) Ogawa, A.; Tomita, N.; Kikuchi, N.; Sando, S.; Aoyama, Y. Aptamer selection for the inhibition of cell adhesion with fibronectin as target. *Bioorg. Med. Chem. Lett.* **2004**, *14*, 4001-4004.

(41) Wang, W. J.; Chen, C. L.; Qian, M. X.; Zhao, X. S. Aptamer biosensor for protein detection using gold nanoparticles. *Anal. Biochem.* **2008**, *373*, 213-219.

(42) Tang, J. J.; Xie, J. W.; Shao, N. S.; Yan, Y. The DNA aptamers that specifically recognize ricin toxin are selected by two in vitro selection methods. *Electrophoresis* **2006**, *27*, 1303-1311.

(43) Bruno, J. G.; Kiel, J. L. In vitro selection of DNA aptamers to anthrax spores with electrochemiluminescence detection. *Biosens. Bioelectron.* **1999**, *14*, 457-464.

(44) Song, K. M.; Lee, S.; Ban, C. Aptamers and their biological applications. *Sensors-Basel.* **2012**, *12*, 612-631.

(45) Zagorovsky, K.; Chan, W. C. W. A Plasmonic DNAzyme strategy for point-of-care genetic detection of infectious pathogens. *Angew. Chem. Int. Edit.* **2013**, *52*, 3168-3171.

(46) Lin, Y. W.; Huang, C. C.; Chang, H. T. Gold nanoparticle probes for the detection of mercury, lead and copper ions. *The Analyst* **2011**, *136*, 863-871.

(47) Yoosaf, K.; Ipe, B. I.; Suresh, C. H.; Thomas, K. G. In situ synthesis of metal nanoparticles and selective naked-eye detection of lead ions from aqueous media. *J. Phys. Chem. C.* **2007**, *111*, 12839-12847.

(48) Hazarika, P.; Ceyhan, B.; Niemeyer, C. M. Reversible switching of DNA-gold nanoparticle aggregation. *Angew. Chem. Int. Edit.* **2004**, *43*, 6469-6471.

(49) Kim, T.; Lee, K.; Gong, M. S.; Joo, S. W. Control of gold nanoparticle aggregates by manipulation of interparticle interaction. *Langmuir* **2005**, *21*, 9524-9528.

(50) Hurst, S. J.; Lytton-Jean, A. K. R.; Mirkin, C. A. Maximizing DNA loading on a range of gold nanoparticle sizes. *Anal. Chem.* **2006**, *78*, 8313-8318.

(51) Wu, S. H.; Wu, Y. S.; Chen, C. H. Colorimetric sensitivity of gold nanoparticles: Minimizing interparticular repulsion as a general approach. *Anal. Chem.* **2008**, *80*, 6560-6566.

(52) Liu, C. W.; Hsieh, Y. T.; Huang, C. C.; Lin, Z. H.; Chang, H. T. Detection of mercury(II) based on Hg(2+)-DNA complexes inducing the aggregation of gold nanoparticles. *Chem. Commun.* **2008**, 2242-2244.

(53) Guan, J.; Jiang, L.; Zhao, L. L.; Li, J.; Yang, W. S. pH-dependent response of citrate capped Au nanoparticle to Pb2+ ion. *Colloid. Surface. A.* **2008**, *325*, 194-197.

(54) Liu, J. W.; Lu, Y. A colorimetric lead biosensor using DNAzyme-directed assembly of gold nanoparticles. *J. Am. Chem. Soc.* **2003**, *125*, 6642-6643.

(55) Liu, J. W.; Lu, Y. Accelerated color change of gold nanoparticles assembled by DNAzymes for simple and fast colorimetric Pb2+ detection. *J. Am. Chem. Soc.* **2004**, *126*, 12298-12305.

(56) Liu, J. W.; Mazumdar, D.; Lu, Y. A simple and sensitive "dipstick" test in serum based on lateral flow separation of aptamer-linked nanostructures". *Angew. Chem. Int. Edit.* **2006**, *45*, 7955-7959.

(57) Liu, J. W.; Lu, Y. Non-base pairing DNA provides a new dimension for controlling aptamer-linked nanoparticles and sensors. *J. Am. Chem. Soc.* **2007**, *129*, 8634-8643.

(58) Petryayeva, E.; Algar, W. R. Toward point-of-care diagnostics with consumer electronic devices: the expanding role of nanoparticles. *Rsc. Adv.* **2015**, *5*, 22256-22282.

(59) Mirkin, C. A.; Letsinger, R. L.; Mucic, R. C.; Storhoff, J. J. A DNA-based method for rationally assembling nanoparticles into macroscopic materials. *Nature* **1996**, *382*, 607-609.

(60) Jin, R. C.; Wu, G. S.; Li, Z.; Mirkin, C. A.; Schatz, G. C. What controls the melting properties of DNA-linked gold nanoparticle assemblies? *J. Am. Chem. Soc.* **2003**, *125*, 1643-1654.

(61) Gibbs-Davis, J. M.; Schatz, G. C.; Nguyen, S. T. Sharp melting transitions in DNA hybrids without aggregate dissolution: Proof of neighboring-duplex cooperativity. *J. Am. Chem. Soc.* **2007**, *129*, 15535-15540.

(62) Maye, M. M.; Nykypanchuk, D.; van der Lelie, D.; Gang, O. A simple method for kinetic control of DNA-induced nanoparticle assembly. *J. Am. Chem. Soc.* **2006**, *128*, 14020-14021.

(63) Lytton-Jean, A. K. R.; Gibbs-Davis, J. M.; Long, H.; Schatz, G. C.; Mirkin, C. A.; Nguyen, S. T. Highly cooperative behavior of peptide nucleic acid-linked DNA-modified gold-nanoparticle and comb-polymer aggregates. *Adv. Mater.* **2009**, *21*, 706-709.

(64) Storhoff, J. J.; Elghanian, R.; Mucic, R. C.; Mirkin, C. A.; Letsinger, R. L. One-pot colorimetric differentiation of polynucleotides with single base

imperfections using gold nanoparticle probes. *J. Am. Chem. Soc.* **1998**, *120*, 1959-1964.

(65) Li, J. S.; Deng, T.; Chu, X.; Yang, R. H.; Jiang, J. H.; Shen, G. L.; Yu, R. Q. Rolling circle amplification combined with gold nanoparticle aggregates for highly sensitive identification of single-nucleotide polymorphisms. *Anal. Chem.* **2010**, *82*, 2811-2816.

(66) Fire, A.; Xu, S. Q. Rolling replication of short DNA circles. *P. Natl. Acad. Sci. USA*. **1995**, *92*, 4641-4645.

(67) Liu, J.; Lu, Y. Stimuli-responsive disassembly of nanoparticle aggregates for light-up colorimetric sensing. *J. Am. Chem. Soc.* **2005**, *127*, 12677-12683.

(68) Zhou, Z. X.; Wei, W.; Zhang, Y. J.; Liu, S. Q. DNA-responsive disassembly of AuNP aggregates: influence of nonbase-paired regions and colorimetric DNA detection by exonuclease III aided amplification. *J. Mater. Chem. B.* **2013**, *1*, 2851-2858.

(69) Trantakis, I. A.; Bolisetty, S.; Mezzenga, R.; Sturla, S. J. Reversible aggregation of DNA-decorated gold nanoparticles controlled by molecular recognition. *Langmuir* **2013**, *29*, 10824-10830.

(70) Sikder, M. D. H.; Gibbs-Davis, J. M. The Influence of gap length on cooperativity and rate of association in DNA-modified gold nanoparticle aggregates. *J. Phys. Chem. C.* **2012**, *116*, 11694-11701.

(71) Smith, B. D.; Dave, N.; Huang, P. J. J.; Liu, J. W. Assembly of DNA-functionalized gold nanoparticles with gaps and overhangs in linker DNA. *J. Phys. Chem. C.* **2011**, *115*, 7851-7857.

(72) Stoeva, S. I.; Lee, J. S.; Thaxton, C. S.; Mirkin, C. A. Multiplexed DNA detection with biobarcoded nanoparticle probes. *Angew. Chem. Int. Edit.* **2006**, *45*, 3303-3306.

(73) Adams, N. M.; Jackson, S. R.; Haselton, F. R.; Wright, D. W. Design, synthesis, and characterization of nucleic-acid-functionalized gold surfaces for biomarker detection. *Langmuir* **2012**, *28*, 1068-1082.

(74) Thaxton, C. S.; Georganopoulou, D. G.; Mirkin, C. A. Gold nanoparticle probes for the detection of nucleic acid targets. *Clin. Chim. Acta.* **2006**, *363*, 120-126.

(75) Laromaine, A.; Koh, L. L.; Murugesan, M.; Ulijn, R. V.; Stevens, M. M. Protease-triggered dispersion of nanoparticle assemblies. *J. Am. Chem. Soc.* **2007**, *129*, 4156-4157.

(76) Kelley, S. O.; Mirkin, C. A.; Walt, D. R.; Ismagilov, R. F.; Toner, M.; Sargent, E. H. Advancing the speed, sensitivity and accuracy of biomolecular detection using multi-length-scale engineering. *Nat. Nanotechnol.* **2014**, *9*, 969-980.

(77) Giljohann, D. A.; Mirkin, C. A. Drivers of biodiagnostic development. *Nature* **2009**, *462*, 461-464.

(78) Huttanus, H. M.; Graugnard, E.; Yurke, B.; Knowlton, W. B.; Kuang, W.; Hughes, W. L.; Lee, J. Enhanced DNA sensing via catalytic aggregation of gold nanoparticles. *Biosens. Bioelectron.* **2013**, *50*, 382-386.

(79) Kibbe, W. A. OligoCalc: an online oligonucleotide properties calculator. *Nucleic Acids Res.* **2007**, *35*, W43-W46.

(80) Grabar, K. C.; Freeman, R. G.; Hommer, M. B.; Natan, M. J. Preparation and characterization of Au colloid monolayers. *Anal. Chem.* **1995**, *67*, 735-743.

(81) Elghanian, R.; Storhoff, J. J.; Mucic, R. C.; Letsinger, R. L.; Mirkin, C. A. Selective colorimetric detection of polynucleotides based on the distance-dependent optical properties of gold nanoparticles. *Science* **1997**, *277*, 1078-1081.

(82) Chen, G. H.; Chen, W. Y.; Yen, Y. C.; Wang, C. W.; Chang, H. T.; Chen, C. F. Detection of mercury(II) ions using colorimetric gold nanoparticles on paper-based analytical devices. *Anal. Chem.* **2014**, *86*, 6843-6849.

(83) Taton, T. A.; Mirkin, C. A.; Letsinger, R. L. Scanometric DNA array detection with nanoparticle probes. *Science* **2000**, *289*, 1757-1760.

(84) Alivisatos, A. P.; Johnsson, K. P.; Peng, X. G.; Wilson, T. E.; Loweth, C. J.; Bruchez, M. P.; Schultz, P. G. Organization of 'nanocrystal molecules' using DNA. *Nature* **1996**, *382*, 609-611.

(85) Bhatt, N.; Huang, P. J. J.; Dave, N.; Liu, J. W. Dissociation and degradation of thiol-modified DNA on gold nanoparticles in aqueous and organic solvents. *Langmuir* **2011**, *27*, 6132-6137.

(86) Volkert, A. A.; Subramaniam, V.; Ivanov, M. R.; Goodman, A. M.; Haes, A. J. Salt-mediated self-assembly of thioctic acid on gold nanoparticles. *Acs Nano* **2011**, *5*, 4570-4580.

(87) Li, F.; Zhang, H. Q.; Dever, B.; Li, X. F.; Le, X. C. Thermal stability of DNA functionalized gold nanoparticles. *Bioconjugate Chem.* **2013**, *24*, 1790-1797.

(88) Yurke, B.; Turberfield, A. J.; Mills, A. P.; Simmel, F. C.; Neumann, J. L. A DNA-fuelled molecular machine made of DNA. *Nature* **2000**, *406*, 605-608.

(89) Srinivas, N.; Ouldridge, T. E.; Sulc, P.; Schaeffer, J. M.; Yurke, B.; Louis, A. A.; Doye, J. P. K.; Winfree, E. On the biophysics and kinetics of toehold-mediated DNA strand displacement. *Nucleic Acids Res.* **2013**, *41*, 10641-10658.

(90) Duan, R. X.; Wang, B. Y.; Hong, F.; Zhang, T. C.; Jia, Y. M.; Huang, J. Y.; Hakeem, A.; Liu, N. N.; Lou, X. D.; Xia, F. Real-time monitoring of enzyme-free strand displacement cascades by colorimetric assays. *Nanoscale* **2015**, *7*, 5719-5725.

(91) Yao, D. B.; Wang, B.; Xiao, S. Y.; Song, T. J.; Huang, F. J.; Liang, H. J. What controls the "Off/On Switch" in the toehold-mediated strand displacement reaction on DNA conjugated gold nanoparticles? *Langmuir* **2015**, *31*, 7055-7061.

(92) Chiu, T. C.; Huang, C. C. Aptamer-functionalized nano-biosensors. *Sensors-Basel.* **2009**, *9*, 10356-10388.

(93) Alladin-Mustan, B. S.; Mitran, C. J.; Gibbs-Davis, J. M. Achieving room temperature DNA amplification by dialling in destabilization. *Chem. Commun.* **2015**, *51*, 9101-9104.

(94) Clerc, O.; Greub, G. Routine use of point-of-care tests: usefulness and application in clinical microbiology. *Clin. Microbiol. Infec.* **2010**, *16*, 1054-1061.

(95) Alkilany, A. M.; Abulateefeh, S. R.; Mills, K. K.; Yaseen, A. I. B.; Hamaly, M. A.; Alkhatib, H. S.; Aiedeh, K. M.; Stone, J. W. Colloidal stability of citrate and mercaptoacetic acid capped gold nanoparticles upon lyophilization: Effect of capping ligand attachment and type of cryoprotectants. *Langmuir* **2014**, *30*, 13799-13808.

(96) Endres, T.; Zheng, M. Y.; Beck-Broichsitter, M.; Kissel, T. Lyophilised ready-to-use formulations of PEG-PCL-PEI nano-carriers for siRNA delivery. *Int. J. Pharmaceut.* **2012**, *428*, 121-124.

(97) Lee, M. K.; Kim, M. Y.; Kim, S.; Lee, J. Cryoprotectants for freeze drying of drug nano-suspensions: Effect of freezing rate. *J. Pharm. Sci-Us.* **2009**, *98*, 4808-4817.

(98) MacCuspie, R. I.; Allen, A. J.; Martin, M. N.; Hackley, V. A. Just add water: reproducible singly dispersed silver nanoparticle suspensions on-demand. *J. Nanopart. Res.* **2013**, *15*, 1760-1769.

(99) Asadishad, B.; Vossoughi, M.; Alamzadeh, I. In vitro release behavior and cytotoxicity of doxorubicin-loaded gold nanoparticles in cancerous cells. *Biotechnol. Lett.* **2010**, *32*, 649-654.

(100) Zhang, L.; Li, P.; Li, D.; Guo, S.; Wang, E. Effect of freeze-thawing on lipid bilayer-protected gold nanoparticles. *Langmuir* **2008**, *24*, 3407-3411.

(101) Randeria, P. S.; Jones, M. R.; Kohlstedt, K. L.; Banga, R. J.; de la Cruz, M. O.; Schatz, G. C.; Mirkin, C. A. What controls the hybridization thermodynamics of spherical nucleic acids? *J. Am. Chem. Soc.* **2015**, *137*, 3486-3489.